Plant, Cell & Environment

Plant, Cell and Environment (2015) doi: 10.1111/pce.12535

Original Article

AtLa1 protein initiates IRES-dependent translation of *WUSCHEL* mRNA and regulates the stem cell homeostasis of *Arabidopsis* in response to environmental hazards

Yuchao Cui[1], Shaofei Rao[1], Beibei Chang[1], Xiaoshuang Wang[1], Kaidian Zhang[1], Xueliang Hou[1], Xueyi Zhu[1], Haijun Wu[2], Zhaoxia Tian[2], Zhong Zhao[2], Chengwei Yang[3] & Tao Huang[1]

[1]State Key Laboratory of Cellular Stress Biology, School of Life Sciences, Xiamen University, Fujian 361102, China[2]School of Life Sciences, University of Science and Technology of China, Hefei, 230027, China[3]Guangdong Key Laboratory of Biotechnology for Plant Development, College of Life Science, South China Normal University, Guangzhou 510631, China

ABSTRACT

Plant stem cells are hypersensitive to environmental hazards throughout their life cycle, but the mechanism by which plants safeguard stem cell homeostasis in response to environmental hazards is largely unknown. The homeodomain transcription factor WUSCHEL (WUS) protein maintains the stem cell pool in the shoot apical meristem of *Arabidopsis*. Here, we demonstrate that the translation of *WUS* mRNA is directed by an internal ribosomal entry site (IRES) located in the 5′-untranslated region. The AtLa1 protein, an RNA-binding factor, binds to the 5′-untranslated region and initiates the IRES-dependent translation of *WUS* mRNA. Knockdown of *AtLa1* expression represses the *WUS* IRES-dependent translation and leads to the arrest of growth and development. The AtLa1 protein is mainly located in the nucleoplasm. However, environmental hazards promote the nuclear-to-cytoplasmic translocation of the AtLa1 protein, which further enhances the IRES-dependent translation of *WUS* mRNA. Genetic evidence indicates that the WUS protein increases the tolerance of the shoot apical meristem to environmental hazards. Based on these results, we conclude that the stem cell niche in *Arabidopsis* copes with environmental hazards by enhancing the IRES-dependent translation of *WUS* mRNA under the control of the AtLa1 protein.

Key-words: translation control; *WUS* mRNA.

INTRODUCTION

Post-embryonic development of plants is dependent on the continual proliferation and differentiation of stem cells in the shoot apical meristem (SAM) and the root apical meristem (RAM). In the SAM of *Arabidopsis*, the homeodomain transcription factor WUS specifies stem cell identity and promotes the proliferation of stem cells (Laux *et al*. 1996; Mayer *et al*. 1998). The WUS is expressed in the organizing centre and transported to the three outermost cell layers of the SAM, where stem cells are located (Yadav *et al*. 2011). The WUS protein also stimulates the expression of *CLAVATA3* (*CLV3*) in the stem cell region, which further interacts with the CLAVATA1-CLAVATA2/CORYNE receptor to restrict the expression level and region of the *WUS* gene (Clark *et al*. 1997; Kayes & Clark 1998; Jeong *et al*. 1999; Müller *et al*. 2008). A negative feedback loop between *WUS* and *CLV3* dynamically maintains the position and size of the stem cell pool in the SAM (Fletcher *et al*. 1999; Brand *et al*. 2000; Schoof *et al*. 2000; Lenhard & Laux 2003). It is generally assumed that stem cell homeostasis is strictly regulated by the WUS protein in response to developmental signals and environmental cues. In contrast to animals, plants cannot escape environmental hazards. Environmental hazards such as drought, high salinity and ultraviolet (UV) irradiation can cause DNA damage and mutation (Bray & West 2005). Previous studies have demonstrated that plant stem cells are hypersensitive to DNA damage caused by environmental hazards (Fulcher & Sablowski 2009; Furukawa *et al*. 2010). Therefore, it is important for plants to maintain stem cell homeostasis in the presence of environmental hazards. The specific responses of the stem cell niche to exposure to environmental hazards remain to be elucidated.

The La protein is a highly expressed RNA-binding factor that is involved in the processing and metabolism of many RNAs in nearly all eukaryotes (Wolin & Cedervall 2002). A typical La protein contains three structured domains: the N-terminal La motif (LAM), a canonical RNA recognition motif (RRM1), and an atypical RNA recognition motif (RRM2) (Maraia & Intine 2001). The La protein transiently binds to the 3′-UUU-OH motif of all polymerase III primary transcripts and the polymerase II-transcribed small RNAs that terminate in a 3′-UUU-OH motif (Stefano 1984; Kufel *et al*. 2000; Wolin & Cedervall 2002; Inada & Guthrie 2004). In addition, the La protein is also involved in the correct folding of certain pre-tRNAs (Chakshusmathi *et al*. 2003), the assembly of U snRNAs into ribonucleoprotein complexes (Pannone *et al*. 1998), and the quality control of newly synthesized non-coding pre-tRNAs (Copela *et al*. 2006; Kadaba *et al*. 2006). The C-terminal domain of La proteins

Correspondence: T. Huang. e-mail: Huangtao@xmu.edu.cn

contains a nuclear localization signal peptide, resulting in the localization of the La protein mainly to the nucleoplasm and, in some cases, to the nucleolus, in association with several precursor RNAs (Simons *et al*. 1996; Broekhuis *et al*. 2000; Maraia 2001; Horke *et al*. 2004a,b). However, the distribution of the La protein is not restricted to the nucleus. It has been reported that the human La protein can shuttle between nucleus and cytoplasm (Fok *et al*. 2006), and a small amount of *Xenopus* La protein is also distributed in the cytoplasm (Cardinali *et al*. 2003). In addition, La can be redistributed to the cytoplasm following exposure to environmental stresses, such as UV irradiation and viral infections (Ayukawa *et al*. 2000; Yocupicio-Monroy *et al*. 2007). Cytoplasmic La can bind to the 5'UTRs and stimulate the internal ribosomal entry site (IRES)-dependent translation of some cellular mRNAs and viral mRNAs (Holcik & Korneluk 2000; Kim *et al*. 2001; Costa-Mattioli *et al*. 2004). Therefore, the La protein can enhance the IRES-dependent translation of certain RNAs in response to environmental hazards.

In *Arabidopsis*, the protein encoded by the At4g32720 locus has been identified as a true La homologue and named AtLa1 (Fleurdépine *et al*. 2007). Similar to the human La protein, AtLa1 contains three structured domains. The AtLa1 protein is mainly distributed in the nucleoplasm and fulfils the nuclear La functions in the maturation and stability of transcripts encoded by RNA polymerase III or RNA polymerase II. In addition, loss-of-function of the *AtLa1* gene arrests embryonic development at an early stage (Fleurdépine *et al*. 2007). However, the function of AtLa1 in *Arabidopsis* development remains to be fully elucidated.

In this study, we demonstrated that the AtLa1 protein is involved in the regulation of stem cell homeostasis in *Arabidopsis*. *WUS* mRNA contains an IRES in its 5'UTR. AtLa1 binds to the 5'UTR and initiates the IRES-dependent translation of *WUS* mRNA. When *Arabidopsis* is subjected to environmental stresses such as UV-B irradiation and radiomimetic drug zeocin, nuclear AtLa1 is redistributed into the cytoplasm and enhances the translation of *WUS* mRNA, further promoting the proliferation of stem cells. Our results clearly demonstrate that stem cell homeostasis in *Arabidopsis* is regulated by the AtLa1 protein in response to environmental hazards.

MATERIALS AND METHODS

Plasmids construction

The CaMV *35S* promoter in the *pH2GW7* vector was replaced with the *STM* promoter (from −5000 bp to the base before the translation start codon) to create *pH2GW7_STM*$_{pro}$. The *WUS* promoter (from −3600 bp to the base before the translation start codon) and 2.5 kb of the 3'downstream fragment (+1697bp–+3296 bp) were ligated to an *AttR1-ccdB-AttR2* cassette and a T35S terminator in the *pHGW* vector to create *pHGW-WUS*$_{pro}$. The *CLV3* promoter (from −1600 bp to the base before the translation start codon) and 1.5 kb of the 3'downstream fragment (+585 bp–+2064 bp) were also cloned into the *pHGW* vector using the same strategy to create *pHGW-CLV3*$_{pro}$. The green fluorescent protein (*GFP*)*:* β-glucuronidase (*GUS*) fusion gene was cloned into the vectors mentioned earlier to create the *STM*$_{pro}$*:GFP:GUS*, *WUS*$_{pro}$*:GFP:GUS*, and *CLV3*$_{pro}$*:GFP:GUS* constructs using LR Clonase (Invitrogen, Carlsbad, CA, USA). The CaMV *35S* promoter in the *pK2GW7* vector was replaced with the *AtLa1* promoter (from −4116 bp to the base before the translation start codon) to create *pK2GW7_AtLa1*$_{pro}$. The *AtLa1* genomic fragment containing the 2.37 kb coding region and 1.75 kb of the 3′ downstream sequence were cloned into the *pDONR201* vector to create *pDONR201_gAtLa1*, which was further used to create *pDONR201_gAtLa1:GFP:GUS* for the in-frame fusion of the *GFP:GUS* with the *AtLa1* gene. The *AtLa1* genomic fragment and the *gAtLa1:GFP:GUS* fusion gene were cloned into *pK2GW7_AtLa1*$_{pro}$ to create the *AtLa1*$_{pro}$*:gAtLa1* and *AtLa1*$_{pro}$*:gAtLa1:GFP:GUS* constructs.

The *AtLa1* cDNA was amplified with *Xba*I (5′-end) and *Spe*I (3′-end) cloning sites and cloned into *pDONR201* to create *pDONR201_AtLa1*, which was further used to create *pDONR201_HA:AtLa1* by inserting the 3 × HA fragment at the unique *Xba*1 site. *pDONR201_AtLa1* was also used to create *pDONR201_AtLa1syn*, which contained synonymous mutations in every codon of the *AtLa1* gene, introduced by site-directed mutagenesis (Toyobo, Tokyo, Japan). The *GFP* gene and the 3 × HA fragment were inserted at the unique *Xba*I site in *pDONR201_AtLa1syn* to create *pDONR201_GFP:AtLa1syn* and *pDONR201_HA:AtLa1syn*, respectively, which were further used to create the *pDONR201_GFP:AtLa1syn*$_{C40}$ and the *pDONR201_HA:AtLa1syn*$_{C40}$ constructs, in which 120 bp of the 3′ end of the *AtLa1syn* gene were deleted using site-directed mutagenesis. Antisense *AtLa1* was also cloned into *pDONR201* to create *pDONR201_anti-AtLa1*. *WUS* cDNA was cloned into *pDONR201* to create *pDONR201_WUS*, which was further used to create *pDONR201_HA:WUS* for the in-frame fusion of the 3 × HA fragment with the *WUS* gene. The *rolD:GFP:T35S* cassette in *pB7WG2D* was removed by digestion with *Hind*III to create *pB7WG2*. These genes harboured in *pDONR201* were cloned into *pK2GW7* or *pB7WG2* to create *35S*$_{pro}$*:AtLa1*, *35S*$_{pro}$*:HA:AtLa1*, *35S*$_{pro}$*:HA:AtLa1syn,* *35S*$_{pro}$*:HA:AtLa1syn*$_{C40}$, *35S*$_{pro}$*:GFP:AtLa1syn*, *35S*$_{pro}$*:GFP:AtLa1syn*$_{C40}$, *35S*$_{pro}$*:anti-AtLa1* and *35S*$_{pro}$*:HA:WUS* constructs.

WUS cDNA containing the 5'UTR was cloned into *pDONR201* to create *pDONR201_5'UTR-WUS*, which was further used to create *pDONR201_5'UTR-Flag:WUS* for the in-frame fusion of the Flag tag (DYKDDDDK) with the *WUS* gene using a site-directed mutagenesis. The *Flag:WUS*Δ fragment lacking 399 bp at the 3′ end was amplified and inserted into the *pDONR201_5'UTR-Flag:WUS* vector to create the dicistronic construct of *pDONR201_Flag:WUS*Δ*-5'UTR-Flag:WUS*, which was further used to create the *pDONR201_T7:Flag:WUS*Δ*-5'UTR-Flag:WUS* vector by inserting a T7 promoter through site-directed mutagenesis. To create the dicistronic construct containing *RFP, GFP* and the *WUS* 5'UTR, the *RFP* coding region, the 5'UTR of *WUS* gene, and the *GFP* coding region were first ligated into

pDONR201, then cloned into *pB7WG2* to create the *35S$_{pro}$:GFP-WUS 5'UTR-RFP* construct. The CaMV 35S promoter in *pK2GW7* was removed by *Xba*I and *Spe*I digestion to create *pK2GW7m*. To create the dicistronic construct containing the *Renilla luciferase* (*RLuc*) and *Firefly luciferase* (*FLuc*) genes in addition to the *WUS* 5'UTR, the *RLuc* gene, *WUS* 5'UTR, and *FLuc* gene were ligated into *pDONR201* to create *pDONR201_RLuc-WUS 5'UTR-FLuc*. The *RLuc-WUS 5'UTR-FLuc* fragment was further cloned into *pB7WG2* and *pK2GW7m* to create the *35S$_{pro}$:RLuc-WUS 5'UTR-FLuc* construct and the promoterless *RLuc-WUS 5'UTR-FLuc* construct, respectively. For *in vitro* transcription of the *WUS* 5'UTR probe, the *WUS* 5'UTR was cloned into *pDONR201* to create *pDONR201_5'UTR*, which was further used to create *pDONR201_T7:5'UTR* by inserting a T7 promoter. The *AtLa1syn* gene was cloned into *pMBP-c* to create *pMBP-c-AtLa1$_{syn}$*, which was further used to create the mutated *AtLa1syn* genes containing the LAM-RRM1, LAM-RRM2, RRM1-RRM2 or RRM2 domain, respectively, using a site-directed mutagenesis kit. All constructs were confirmed by sequencing. The primer sequences used for plasmid construction are available upon request.

Plant materials and transformation

All constructs in binary vectors were introduced into *Agrobacterium tumefaciens* strain pMP90 and transformed into Col-0 wild-type plants using the floral-dip method (Clough & Bent 1998). Three independent transgenic lines were used for all subsequent analyses. The *atla1 1–2* mutant and the *35S$_{pro}$:Collin:RFP* transgenic plants were obtained from the European *Arabidopsis* Stock Centre. The *WUS$_{pro}$:WUS:GFP CLV3$_{pro}$:mcherry:NLS wus* transgenic plant was kindly provided by Prof. Jan Lohmann. All plants were grown in soil at 22 °C for long days (16 h light/8 h dark) with white fluorescent light (120 μmol m^{-2} s^{-1}).

UV-B irradiation

UV-B light was provided by two 20 W narrowband UV-B tubes (TL20W/01RS; Philips, Eindhoven, The netherlands) as described previously (Biedermann & Hellmann 2010). The rosette leaves of 3-week-old transgenic plants were turned over and irradiated with UV-B light for 2.5 h, then transferred to darkness for 24 h before examining the fluorescence intensity in epidermal cells.

Zeocin treatment

The *35S$_{pro}$:GFP:AtLa1syn* seedlings and *35S$_{pro}$:GFP-WUS 5'UTR-RFP* seedlings were incubated in a zeocin solution as indicated under continuous light for 24 h before examining fluorescence intensity. Seedlings incubated in phosphate-buffered saline (PBS) were used as a control. To examine the effects of zeocin treatment on *WUS* expression in the SAM, the seeds were germinated and grown on a half Murashige and Skoog medium containing different concentrations of zeocin at 22 °C for long days (16 h light/8 h dark) with white fluorescent light (120 μmol m^{-2} s^{-1}).

Protein purification

The *pMBP-c* vectors harbouring the *AtLa1* gene were transformed into *Escherichia coli* BL21. The expression of the maltose-binding protein (MBP) fusion proteins was induced by isopropyl β-D-1-thiogalactopyranoside (IPTG), and the MBP fusion proteins were purified using amylose resin (Bio-Labs, Rawalpindi, Pakistan). The eluted MBP fusion proteins were dialysed against the buffer [16 mM N-(2-hydroxyethyl)piperazine-N′-(2-ethanesulphonic acid) (HEPES)-KOH pH 7.5, 50 mM KCl, 0.5 mM DTT, 0.1 mM ethylenediaminetetraacetic acid (EDTA), 10% glycerol].

In vitro transcription and translation

The *pDONR201_T7:5'UTR* and *pDONR201_T7:Flag:WUS*Δ*-5'UTR-Flag:WUS* vectors were linearized with *Hind*III. The linearized DNAs were purified by phenol/chloroform extraction and ethanol precipitation. Transcription reactions were performed with T7 RNA polymerase according to the manufacturer's instruction (Ambion, Austin, TX, USA). The MBP:AtLa1 protein was added to 50 μL reaction mixtures of the rabbit reticulocyte lysate (RRL) translation system (Promega, Madison, WI, USA) containing 400 ng of *Flag:WUS*Δ*-5'UTR-Flag:WUS* mRNA. At least three independent assays were performed with similar results.

Electrophoretic mobility shift assay (EMSA)

EMSA reactions were performed in a total volume of 20 μL of binding buffer (20 mM Hepes-KOH pH 7.9, 100 mM KCl, 2 mM DTT, and 20% glycerol) containing 60 ng of *in vitro* transcribed *WUS* 5'UTR probe and different concentrations of MBP:AtLa1 protein at 22 °C for 30 min. The EMSA reaction products were resolved on 6% polyacrylamide gels. After electrophoresis, the gel was stained with SYBR® Green EMSA staining solution using an EMSA kit (E33075, Invitrogen).

RNA immunoprecipitation (RIP)

For RIP, nuclear extraction was performed with 10-day-old seedlings (5.0 g) according to an earlier report (Terzi & Simpson 2009). For each immunoprecipitation, 20 μL of Dynabeads® protein A (Invitrogen) coupled to an anti-HA antibody (Santa Cruz Biotechnology, Inc., Santa Cruz, CA, USA) or an anti-c-Myc antibody (Santa Cruz Biotechnology, Inc.) was incubated with 60 μL of nuclear extract overnight at 4 °C under rotation. The supernatants were removed, and the beads were washed four times with PBS (pH 7.4) containing 1% Triton X-100. The immunoprecipitated mRNA was released from the beads by washing with 20 μL of glycine (50 mM, pH 2.8). The *WUS* mRNA in the final wash buffer was examined by RT-PCR to ensure thorough removal of unbound material.

Protein immunoprecipitation

35S$_{pro}$:HA:AtLa1syn seedlings (0.5 g) were homogenized with liquid nitrogen and solubilized in 0.4 mL of extraction buffer

(25 mM Tris-HCl, pH 8.0, 150 mM NaCl, 5% glycerol, 0.05% v/v NP-40, 2.5 mM EDTA and 1 mM phenylmethylsulfonyl fluoride). The homogenates were sequentially centrifuged at 1000 *g* for 10 min, 3000 *g* for 10 min, and 12 000 *g* for 10 min at 4 °C to remove nuclear and cellular debris. Then, the supernatant was mixed with 30 μL of Dynabeads® protein A coupled to an anti-HA antibody overnight at 4 °C with rotation. The beads were washed four times with extraction buffer and then eluted with 25 μL of glycine (50 mM, pH 2.8).

Semi-quantitative RT-PCR and qRT-PCR analysis

Total RNA was extracted using PureLink Plant RNA Reagent (Invitrogen) from 5-day-old seedlings. Total RNAs were treated with DNaseI (Thermo, Massachusetts, USA) to remove any genomic DNA contamination. The isolated RNA was reverse-transcribed in a 20 μL reaction mixture using a cDNA synthesis kit (Toyobo) according to the manufacturer's instructions. qRT-PCR was performed with a CFX96 Touch™ real-time PCR detection system (Bio-Rad, Hercules, CA, USA) with a SYBR *Premix Ex Taq* II kit (Takara Bio, Kyoto, Japan). Three replicate assays were performed with independent RNA samples. Mock RT-PCR was performed to exclude possible genomic DNA contamination. All primers used for RT-PCR analysis are listed in Supporting Information Table S1.

RNA *in situ* hybridization

The expression of *WUS* mRNA and *CLV3* mRNA were analysed by *in situ* hybridization as previously described with minor modifications (Zhao *et al*. 2010).

Immunoblot analysis

Immunoblot analysis was performed using the Protein Detector™ Western Blot kit (KPL, Gaithersburg, Maryland, USA) according to the manufacturer's instructions. The following primary antibodies were used: mouse anti-HA monoclonal antibody (1:250; Santa Cruz Biotechnology, Inc.), mouse anti-Actin antibody (1:2000; Sigma, St Louis, MO, USA), and mouse anti-Flag antibody (1:1000; Sigma). The signal was visualized using a ChemiDoc XRS molecular imaging system (Bio-Rad).

Histochemical localization of GUS activity

The histological analysis of GUS enzyme activity was performed as described by Jefferson *et al.* (1987). At least three independent transgenic lines were used for GUS staining with similar results.

Fluorescence analysis

GFP fluorescence and RFP fluorescence were obtained using excitation/emission values of 488 nm/495–545 nm and 561 nm/578–636 nm, respectively, with a confocal laser scanning microscope (Zeiss LSM 780/Carl Zeiss Meditec AG, Goeschwitzer Strasse 51-52, 07745 Jena, Germany). All samples were examined using the identical microscope settings in every experiment. To examine the fluorescence in the SAM, the shoot apexes were fixed in 7% agarose at 4 °C for 15 min, and sections (50 μm) were then made using a vibrating-blade microtome (KD-400, Ningbo Jiangnan Instrument Factory/Ningbo City, Zhejiang Province, China). At least two independent lines were examined.

Luciferase activity assay

RLuc and FLuc activities were examined using the Dual Luciferase reporter assay kit (Promega) according to the manufacturer's instruction. The data are presented as the averages from assays of at least six independent transgenic lines.

Accession numbers

Sequence data from this paper can be found in the *Arabidopsis* Genome Initiative under the following accession numbers: *WUS* (At2g17950), *CLV3* (At2g27250), *STM* (At1g62360) and *AtLa1* (At4g32720).

RESULTS

Expression pattern of the *AtLa1* gene

An 8.2 kb genomic fragment containing the putative promoter region, open reading frame, and 3′ downstream region of the *AtLa1* gene was cloned and introduced into the heterozygous *atla1-2* mutant. Many homozygous *atla1-2* mutants were identified among the segregating transgenic progenies, suggesting that this 8.2 kb genomic fragment might fully rescue the arrest of embryonic development in the homozygous *atla1-2* mutant (Fleurdépine *et al*. 2007). To monitor the expression pattern of the *AtLa1* gene, we used this 8.2 kb genomic fragment to create the $AtLa1_{pro}$*:gAtLa1:GFP:GUS* construct by fusing the *GFP* gene and the *GUS* gene in frame with the coding region of the *AtLa1* gene (Fig. 1a). The expression of the *AtLa1* gene was examined during the embryogenesis of $AtLa1_{pro}$*:gAtLa1:GFP:GUS* plants. The *AtLa1* gene was universally expressed from the global stage to the mature stage of embryo development (Fig. 1b–f). After germination, the *AtLA1* gene was universally expressed in the cotyledons, leaves, SAM and root (Fig. 1g–i). During the reproductive development stage, the *AtLa1* gene was also expressed in the flowers, particularly in the gynoecium (Fig. 1j–m). These results demonstrated the universal expression of the *AtLa1* gene in different organs at different developmental stages of *Arabidopsis*.

AtLa1 gene is involved in the maintenance of the SAM

Because the loss-of-function of the *AtLa1* gene arrests embryonic development (Fleurdépine *et al*. 2007), we explored the function of the *AtLa1* gene by over expressing it under the control of the CaMV 35S promoter. The growth

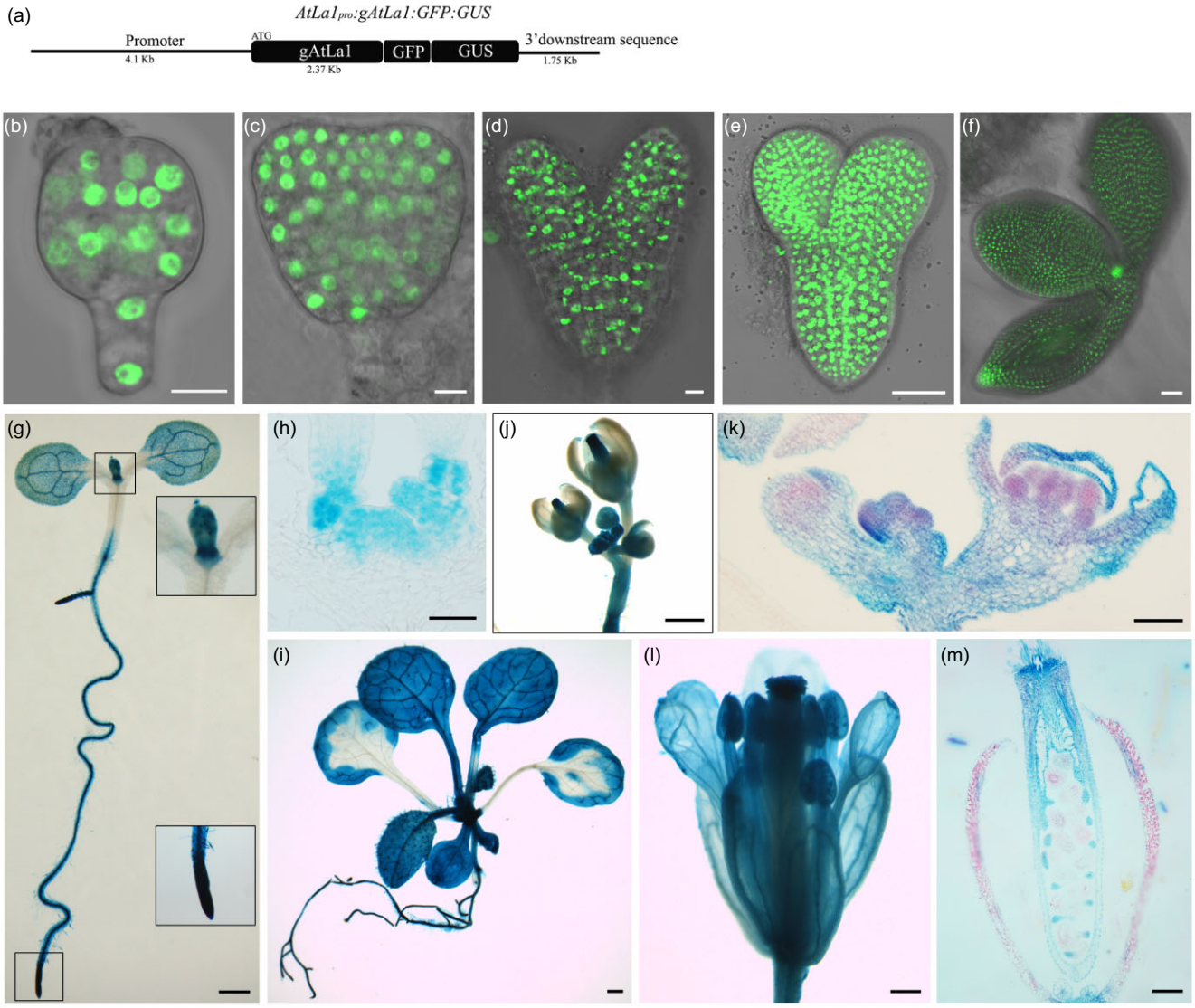

Figure 1. The expression pattern of the *AtLa1* gene in *Arabidopsis*. (a) Diagram of the *AtLa1*$_{pro}$*:gAtLa1:*green fluorescent protein (*GFP*)*:β*-glucuronidase (*GUS*) construct. (b–f) Expression of the *AtLa1* gene at the global stage (b), heart stage (c), torpedo stage (d), linear cotyledon (e) and mature stage (f) during the embryogenesis of the *AtLa1*$_{pro}$*:gAtLa1:GFP:GUS* plant. (g–i) Expression of the *AtLa1* gene in a 5-day-old seedling (g) [inserts are the magnification of shoot apical meristem (SAM) and root apical meristem (RAM), respectively], a 3-week-old seedling (i) and its meristem (h). (j–m) Expression of the *AtLa1* gene in the infloresence (j) and its meristem (k), the flower (l) and gynoecium (m) during the reproductive development stage. Scale bars = 10 μm in b, c and d; 50 μm in e, f, h and k; 500 μm in g, i, j, l and m.

of most of the *35S*$_{pro}$*:AtLa1* lines were significantly repressed after germination. From a total 1638 independent transgenic lines, ~ 18% of lines displaying a strong phenotype failed to develop any rosette leaves after germination (Fig. 2, compare 2b with 2a) and lost the typical dome structure of the SAM (Fig. 2, compare 2c with 2d). ~24% of lines displaying a moderate phenotype finally developed aberrant rosette leaves after several weeks of growth cessation (Fig. 2e). These moderate lines also showed the irregular position of siliques (Fig. 2f). ~35% of lines displaying a weak phenotype only underwent a transient growth cessation during the first week after germination, and then grew normally as the WT plants.

We also created *35S*$_{pro}$*:HA:AtLa1* transgenic plants to monitor the expression level of the HA:AtLa1 protein. The over expression of the HA-tagged AtLa1 protein also inhibited the growth and development of the transgenic plants. Immunoblots revealed that HA:AtLa1 protein levels decreased to an extremely low level in the strong *35S*$_{pro}$*:HA:AtLa1* lines that displayed severe growth cessation. The HA:AtLa1 protein accumulated at a relatively lower level in the moderate lines compared with the WT-like lines (Fig. 2g). These results demonstrated that growth cessation correlated with the decrease in the HA:AtLa1 protein, possibly because of the co-suppression caused by the over

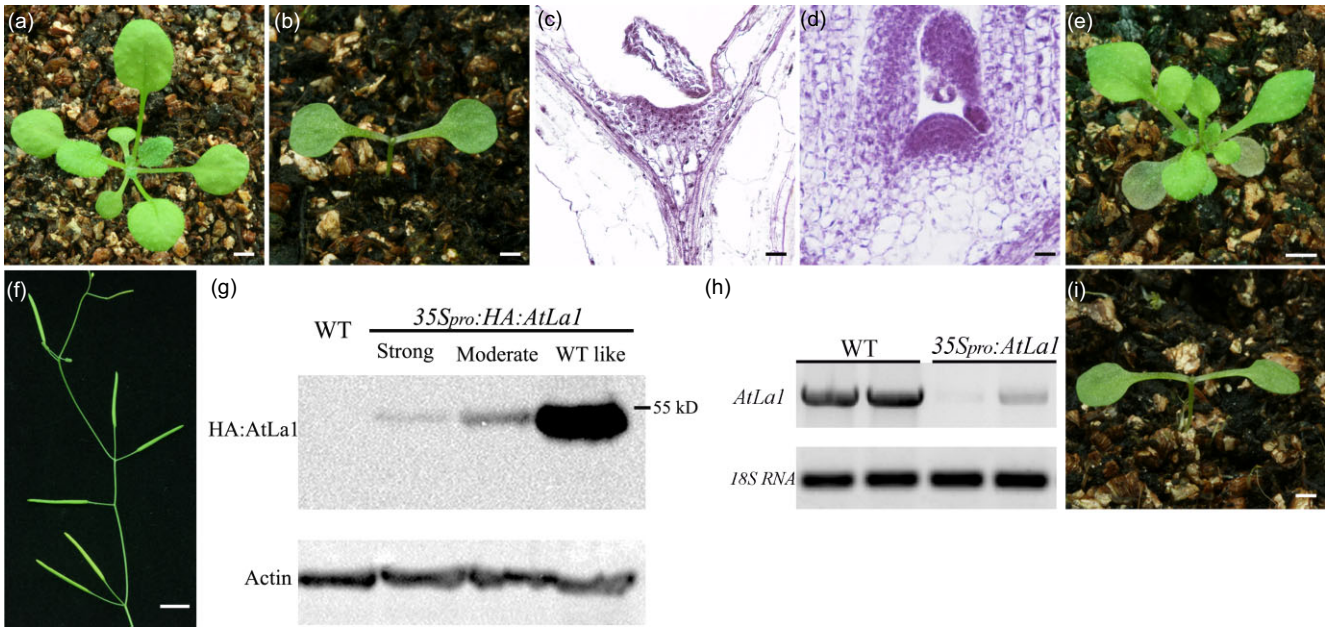

Figure 2. The *AtLa1* gene is involved in shoot apical meristem (SAM) maintenance in *Arabidopsis*. (a) WT plant. (b–d) $35S_{pro}$*:AtLa1* seedlings exhibiting a strong phenotype failed to produce true leaves (b) and lost the typical dome structure of the SAM (c) compared with wild-type (WT) plants (d). (e) $35S_{pro}$*:AtLa1* seedlings exhibiting a moderate phenotype produced aberrant leaves after several weeks of growth cessation. (f) The irregular position of siliques in a $35S_{pro}$*:AtLa1* plant. (g) HA:AtLa1 protein levels gradually decreased in $35S_{pro}$*:HA:AtLa1* lines with moderate and strong phenotypes compared to WT-like lines because of co-suppression. WT was used as a control. (h) The endogenous *AtLa1* mRNA significantly decreased in $35S_{pro}$*:AtLa1* plants compared with WT plants because of co-suppression. (i) The phenotype of the $35S_{pro}$*:anti-AtLa1* plants was similar to that of the $35S_{pro}$*:AtLa1* plants in (b). Scale bars = 0.5 cm in a and e, 2 mm in b and i, 20 μm in c and d, and 1 cm in f.

expression of the *AtLa1* gene. The endogenous *AtLa1* mRNA also significantly decreased in these transgenic plants displaying growth cessation compared with the WT plants because of the co-suppression (Fig. 2h). Clearly, the over expression of *AtLa1* gene in the presence of the universally expressed endogenous *AtLa1* gene always causes the co-suppression in transgenic plants. Furthermore, knockdown of *AtLa1* expression by over expression of the antisense *AtLa1* gene also caused severe growth cessation in $35S_{pro}$*:anti-AtLa1* plants (Fig. 2i). Taken together, these results indicate that the *AtLa1* gene is involved in SAM maintenance.

AtLa1 protein regulates *WUS* expression at the translational level

WUS protein plays an important role in SAM maintainance and the SAM of *wus* mutant fails to develop normally (Laux *et al.* 1996). Because the knockdown of *AtLa1* expression in transgenic plants causes a phenotype similar to that of *wus* mutant, we introduced the $35S_{pro}$*:AtLa1* and $35S_{pro}$*:anti-AtLa1* constructs into one WUS_{pro}*:GFP:GUS* line to explore the possible function of the *AtLa1* gene in *WUS* expression. The over expression of *AtLa1* gene in $35S_{pro}$*:AtLa1* WUS_{pro}*:GFP:GUS* plants also caused the co-suppression of *AtLa1* gene. *GUS* activity was completely absent from the SAM in most of the $35S_{pro}$*:AtLa1* WUS_{pro}*:GFP:GUS* and $35S_{pro}$*:anti-AtLa1* WUS_{pro}*:GFP:GUS* lines, which exhibited varying degrees of growth cessation (Fig. 3b & c). These results suggest that *WUS* expression decreased to an extremely low level upon interference with the expression of the *AtLa1* gene. The previous studies demonstrated that the negative feedback loop between *WUS* and *CLV3* dynamically maintains the stem cell pool in the SAM (Fletcher *et al.* 1999; Brand *et al.* 2000; Schoof *et al.* 2000; Lenhard & Laux 2003). We also explored the effect of the *AtLa1* gene on *CLV3* expression by introducing the $35S_{pro}$*:AtLa1* construct into one $CLV3_{pro}$*:GFP:GUS* line. The GUS activity was also absent from the SAM of the $35S_{pro}$*:AtLa1* $CLV3_{pro}$*:GFP:GUS* plants, which exhibited growth cessation (Fig. 3e). Consistently, *CLV3* mRNA was significantly decreased in the $35S_{pro}$*:AtLa1* WUS_{pro}*:GFP:GUS* and $35S_{pro}$*:anti-AtLa1* WUS_{pro}*:GFP:GUS* plants compared with the control WUS_{pro}*:GFP:GUS* plants (Fig. 3f). The down-regulation of *CLV3* expression might be due to the decrease in the level of WUS protein, which is supposed to stimulate *CLV3* expression (Yadav *et al.* 2011). By contrast, the levels of *GFP:GUS* mRNA and endogenous *WUS* mRNA were significantly increased in these transgenic plants (Fig. 3f), possibly because the *WUS* promoter was released from the feedback inhibition imposed by the CLV3 protein. The RNA *in situ* hybridization also showed that the *WUS* mRNA, but not the *CLV3* mRNA is clearly detected in the inflorescence meristem of $35S_{pro}$*:AtLa1* WUS_{pro}*:GFP:GUS* plants and $35S_{pro}$*:anti-AtLa1* WUS_{pro}*:GFP:GUS* plants displaying a moderate phenotype (Supporting Information Fig. S1). These results suggest that the knockdown of *AtLa1* expression

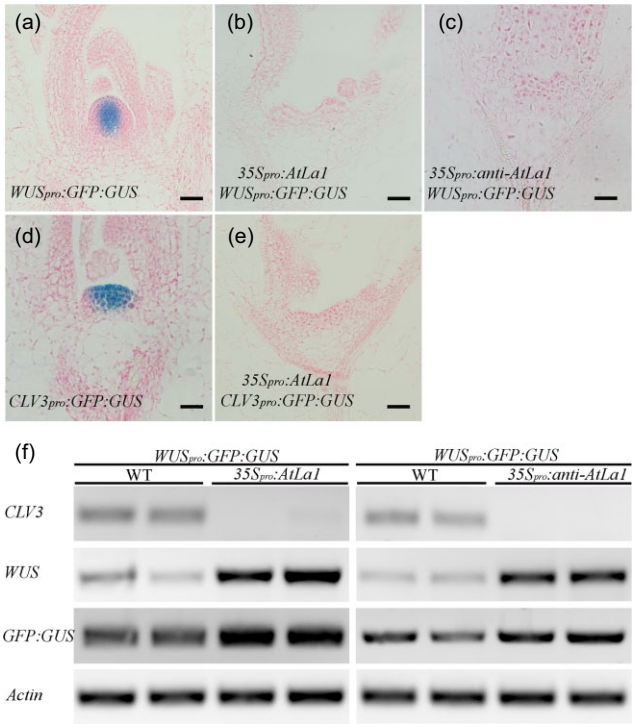

Figure 3. The AtLa1 protein initiates *WUS* 5′UTR-directed translation. (a–c) Translation of the green fluorescent protein (*GFP*):*β*-glucuronidase (*GUS*) mRNA in the shoot apical meristem (SAM) of $35S_{pro}$*:AtLa1* WUS_{pro}*:GFP:GUS* plants (b) and $35S_{pro}$*:anti-AtLa1* WUS_{pro}*:GFP:GUS* plants (c) was significantly repressed compared with the control WUS_{pro}*:GFP:GUS* plants (a) because of the decreased AtLa1 protein expression. GUS activity was visualized using blue colour. (d, e) The GFP:GUS protein was significantly decreased in the SAM of $35S_{pro}$*:AtLa1* $CLV3_{pro}$*:GFP:GUS* plants (e) compared with the control $CLV3_{pro}$*:GFP:GUS* plants (d). Scale bars = 30 *μ*m in a, b, c, d and e. (f) Analysis of the *CLV3*, *WUS* and *GFP:GUS* mRNAs in the $35S_{pro}$*:AtLa1* WUS_{pro}*:GFP:GUS* plants and the $35S_{pro}$*:anti-AtLa1* WUS_{pro}*:GFP:GUS* plants compared with the control WUS_{pro}*:GFP:GUS* plants. At least two independent lines were analysed.

might only inhibit the translation of *GFP:GUS* mRNA and endogenous *WUS* mRNA, which contain the same untranslated regions (UTRs). As a control experiment, the introduction of the $35S_{pro}$*:AtLa1* construct into a STM_{pro}*:GFP:GUS* plant also caused severe growth cessation, but failed to abolish the *STM* expression, as demonstrated by GUS staining (Supporting Information Fig. S2).

AtLa1 protein binds to the 5′UTR of the *WUS* mRNA

Because the AtLa1 protein mainly functions as an RNA-binding protein and plays a possible role in the translation of *WUS* mRNA, we further explored whether the AtLa1 protein could bind to the *WUS* mRNA. To avoid the co-suppression of the *AtLa1* gene, the sequence of the *AtLa1* coding region was synonymously substituted to create the *AtLa1syn* gene (Supporting Information Fig. S3). The $35S_{pro}$*:HA:AtLa1syn* transgenic plant was further created to test the binding of the HA:AtLa1 protein to endogenous *WUS* mRNA in RIP analysis using an anti-HA antibody. The introduction of the $35S_{pro}$*:HA:AtLa1syn* construct into WUS_{pro}*:GFP:GUS* plants did not inhibit the GUS activity in the SAM or the post-embryonic growth of the transgenic plants. The endogenous *WUS* mRNA reproducibly co-immunoprecipitated with the HA:AtLa1 protein in the extracts prepared from $35S_{pro}$*:HA:AtLa1syn* plants using an anti-HA antibody. By contrast, the *WUS* mRNA did not co-immunoprecipitate with the HA:AtLa1 protein using an anti-Myc antibody (Fig. 4a). As another control experiment, the endogenous *STM* mRNA did not co-immunoprecipitate with the HA:AtLa1 protein using an anti-HA antibody either (Fig. 4a). Therefore, it seems that the HA:AtLa1 protein specifically binds to the *WUS* mRNA. The binding of the AtLa1 protein to the 5′UTR of *WUS* mRNA was further examined using an EMSA. The intact AtLa1 protein and the truncated AtLa1 proteins containing the LAM-RRM1, LAM-RRM2, RRM1-RRM2, or RRM2 domain in fusion with MBP were expressed and purified (Fig. 4b). The addition of the MBP-fused AtLa1 protein or just MBP-fused RRM2 domain resulted in a slower migration of the *WUS* 5′UTR probe (Fig. 4c), suggesting that the RRM2 domain of AtLa1 protein can directly bind to the 5′UTR of *WUS* mRNA.

AtLa1 protein initiates the *WUS* IRES-dependent translation *in vitro* and *in vivo*

A subset of mRNAs uses the IRES-dependent translation instead of the 5′terminal cap-dependent translation (Hellen & Sarnow 2001). It was reported that the La protein can bind to the 5′UTR of *Bip* mRNA and mediate the IRES-dependent translation (Kim *et al*. 2001). We also test whether the AtLa1 protein can mediate the IRES-dependent translation of *WUS* mRNA by binding to its 5′UTR. We created a dicistronic construct to transcribe the capped *Flag:WUSΔ-5′UTR-Flag:WUS* mRNA for the *in vitro* cap-dependent translation of a truncated Flag:WUSΔ protein lacking the C-terminal 133 amino acids and to test the possible cap-independent translation of the Flag:WUS protein (Fig. 5a). The RRL translation system was used to examine the existence of an IRES in the 5′UTR of the *WUS* mRNA and the involvement of the AtLa1 protein in *WUS* IRES-dependent translation. If the *WUS* 5′UTR contains an IRES and mediates the translation of second cistron, the Flag:WUS protein should be produced in the RRL translation system. *In vitro* translation of the capped *Flag:WUSΔ-5′UTR-Flag:WUS* mRNA was performed by adding increasing amounts of purified MBP:AtLa1 protein. The translation of second cistron was significantly enhanced by the addition of the MBP:AtLa1 protein, but not by the addition of MBP (Fig. 5b). These results indicate that the *WUS* 5′UTR contains an IRES that mediates the cap-independent translation and that the AtLa1 protein initiates *WUS* IRES-dependent translation in a dose-dependent manner.

We also used the sensitive reporter assay to examine the *WUS* IRES-dependent translation of luciferase in transgenic

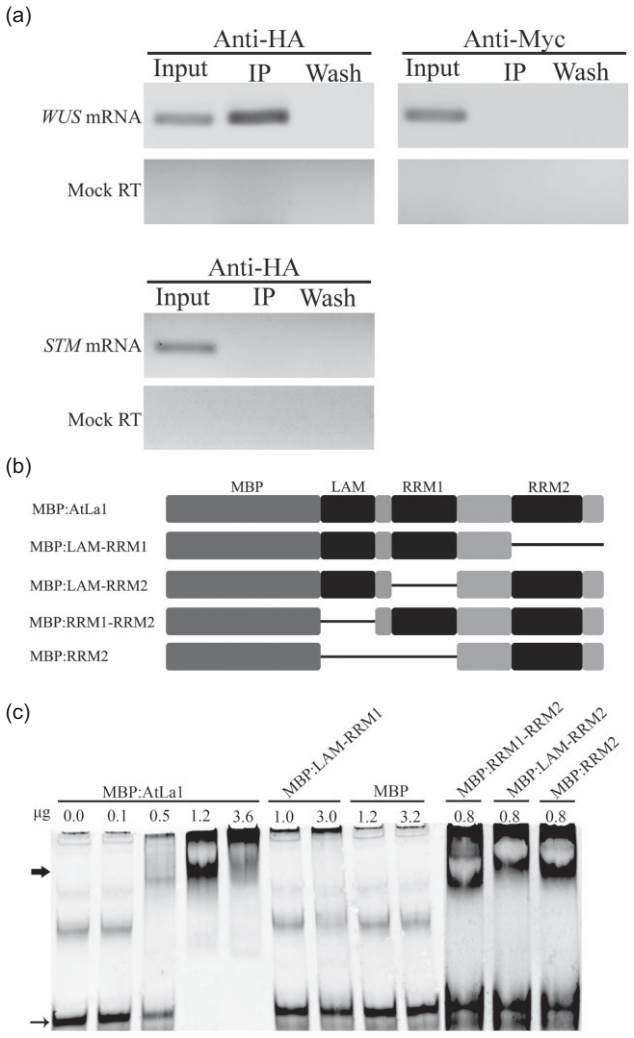

Figure 4. The AtLa1 protein binds to the 5′UTR of the *WUS* mRNA. (a) The *WUS* mRNA co-immunoprecipitates with the HA:AtLa1 protein from *35S$_{pro}$:HA:AtLa1syn* plants using an anti-HA antibody, but not an anti-Myc antibody. The STM mRNA does not co-immunoprecipitate with the HA:AtLa1 protein using an anti-HA antibody either. (b) A schematic diagram of the intact AtLa1 protein and the truncated AtLa1 proteins containing different domains in fusion with maltose-binding protein (MBP). The lines indicate the deleted domains. (c) The MBP:AtLa1, MBP:LAM-RRM2, MBP:RRM1-RRM2, and MBP:RRM2 proteins, but not the MBP:LAM-RRM1 protein, bind to the *WUS* 5′UTR in EMSA analysis. MBP was used as a control protein. The thick arrow indicates the protein–RNA complex. The thin arrow indicates the position of the free *WUS* 5′UTR probe.

plants carrying the dicistronic *35S$_{pro}$:RLuc-WUS 5'UTR-FLuc* construct (Fig. 5a). The enzymatic activity of FLuc was significantly higher than that of RLuc (Fig. 5c), demonstrating the *WUS* IRES-dependent translation of FLuc. When the *35S$_{pro}$:AtLa1* construct was introduced into *35S$_{pro}$:RLuc-WUS 5'UTR-FLuc* plants to induce the co-suppression of *AtLa1* gene, the enzymatic activity of FLuc was significantly decreased (Fig. 5c). Clearly, the *WUS* IRES-dependent translation of FLuc is regulated by the level of AtLa1 protein. It is necessary to determine whether the intercistronic spacer region can provide a cryptic promoter activity when the dicistronic construct is used to identify an IRES-dependent translation (Hellen & Sarnow 2001). To determine whether the *WUS* 5'UTR contains a cryptic promoter, we created transgenic plants carrying a promoterless *RLuc-WUS 5'UTR-FLuc* construct (Fig. 5a). The enzymatic activities of FLuc and RLuc in the independent transgenic lines were significantly decreased to the level detected in WT plants (Fig. 5c). These results indicate that the *WUS* 5'UTR has no cryptic promoter activity.

Environmental hazards enhance the nuclear-to-cytoplasmic translocation of the AtLa1 protein

The AtLa1 protein is mainly located in the nucleoplasm, but is occasionally distributed in the nuclear cavity in isolated protoplasts (Fleurdépine *et al.* 2007). We observed a similar distribution of the AtLa1:GFP:GUS protein in the root cells of *AtLa1$_{pro}$:gAtLA1:GFP:GUS* plants (Supporting Information Fig. S4). The human La protein can be cleaved by caspase at the DXXD motif in the C-terminus; the cleaved protein is then trafficked from the nucleus to the cytoplasm of HL-60 cells (Ayukawa *et al.* 2000). Because the cleaved HA:AtLa1 protein was not clearly detected by immunoblot in the total protein prepared from the *35S$_{pro}$:HA:AtLa1syn* seedlings (Fig. 6b, lane 1), the cytoplasmic proteins were prepared, and HA:AtLa1 was concentrated by immunoprecipitation using an anti-HA antibody. One smaller HA:AtLa1 protein was detected (Fig. 6b, lane 2), suggesting that only a small amount of the HA:AtLa1 protein might be cleaved in its C-terminus and traffic to cytoplasm. The AtLa1 protein also contains a possible ^{394}DRFD^{397} cleavage site in its C-terminus; cleavage at this site would remove the 40 C-terminal amino acids of the protein. We created *35S$_{pro}$:HA:AtLa1syn$_{C40}$* transgenic plants, which express the truncated HA:AtLa1$_{C40}$ protein lacking these 40 C-terminal amino acids (Fig. 6a). However, the cleaved HA:AtLa1 protein was 2–3 kDa smaller than the HA:AtLa1$_{C40}$ protein (Fig. 6b, lane 3), suggesting that the AtLa1 protein might be cleaved of 60–70 C-terminal amino acids. Therefore, the cleavage mechanism of the AtLa1 protein might differ from that of the human La protein.

To examine the subcellular localization of the AtLa1 protein, the *35S$_{pro}$:GFP:AtLa1syn* construct (Fig. 6a) was introduced into *35S$_{pro}$:Collin:RFP* plants, in which the constitutively expressed Collin:RFP protein is localized to the Cajal Bodies within the nucleus (Collier *et al.* 2006). The GFP:AtLa1 protein was found to be exclusively localized to the nucleus and colocalized with the Collin:RFP protein in epidermal cells after we have extensively examined all independent lines (Fig. 6c), suggesting that the over expression of GFP:AtLa1 protein did not cause a clear diffusion in its subcellular localization. Cytoplasmic GFP:AtLa1 was not observed, possibly because only a small amount of GFP:AtLa1 protein might be cleaved in its C-terminus and traffic to cytoplasm. To further examine the involvement of the C-terminal domain of the AtLa1 protein in subcellular localization, we created a *35S$_{pro}$:GFP:AtLa1syn$_{C40}$* transgenic plant, which expresses the GFP:AtLa1$_{C40}$ protein lacking the

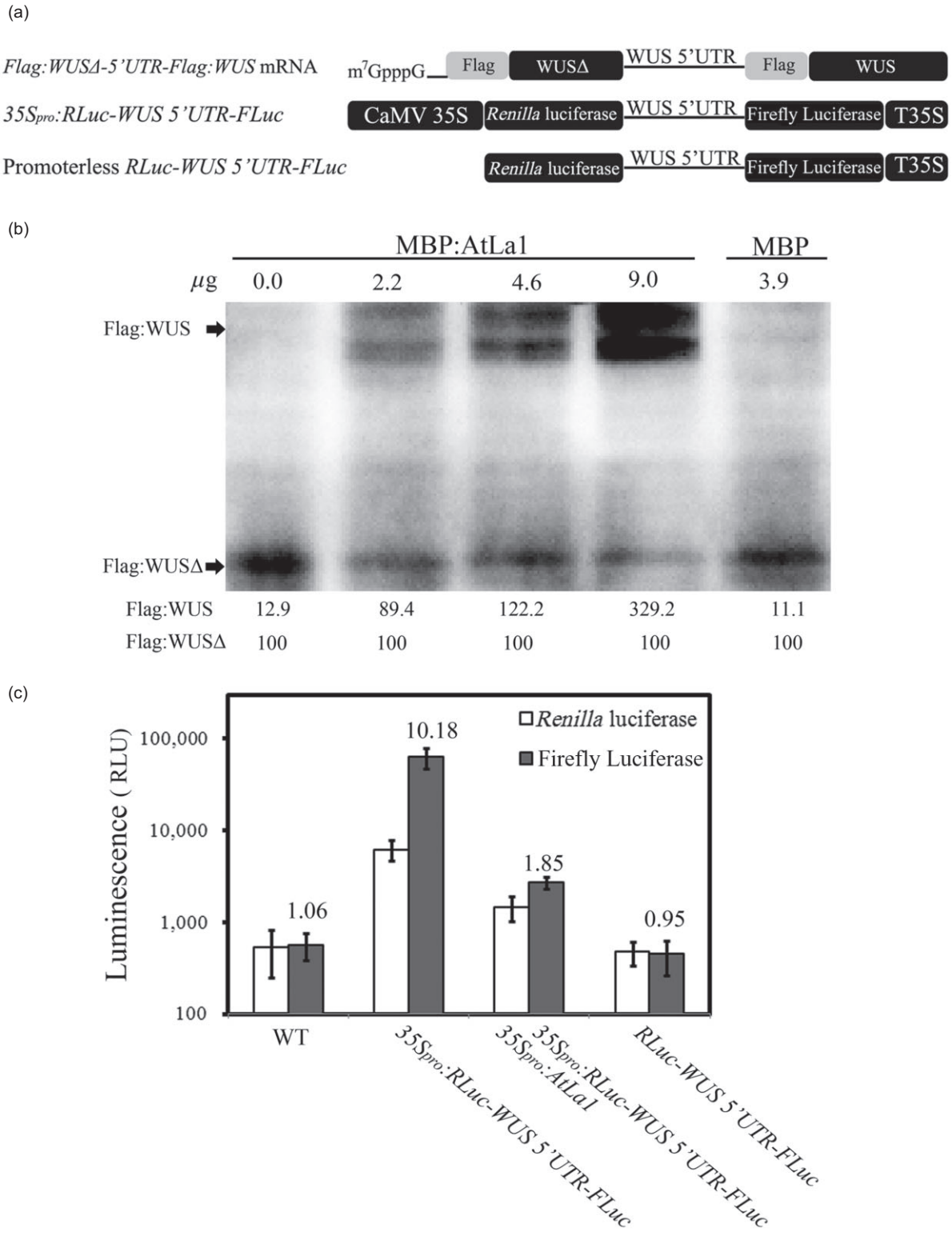

Figure 5. The AtLa1 protein initiates *WUS* IRES-dependent translation *in vitro* and *in vivo*. (a) A schematic diagram of the capped *Flag:WUSΔ-5'UTR-Flag:WUS* mRNA in which the *WUSΔ* in the first cistron is 399 bp shorter than *WUS*, and the $35S_{pro}$*:RLuc-WUS 5'UTR-FLuc* construct and promoterless *RLuc-WUS 5'UTR-FLuc* construct. (b) *In vitro* translation of the *Flag:WUSΔ-5'UTR-Flag:WUS* mRNA was performed by adding increasing amounts of the MBP:AtLa1 fusion protein to the reaction mixtures. MBP was used as the control protein. The relative efficiencies of *WUS* IRES-directed translation were normalized to the cap-dependent translation, which was set to an arbitrary value of 100. (c) The enzymatic activities of *Renilla* luciferase (RLuc) and firefly luciferase (FLuc) in wild-type (WT) plants and the transgenic plants carrying the $35S_{pro}$*:RLuc-WUS 5'UTR-FLuc* construct or promoterless *RLuc-WUS 5'UTR-FLuc* construct (data presented are mean ± SE, $n = 6$). The relative ratio of FLuc/RLuc in different plants was also marked above the columns. RLU, relative light units.

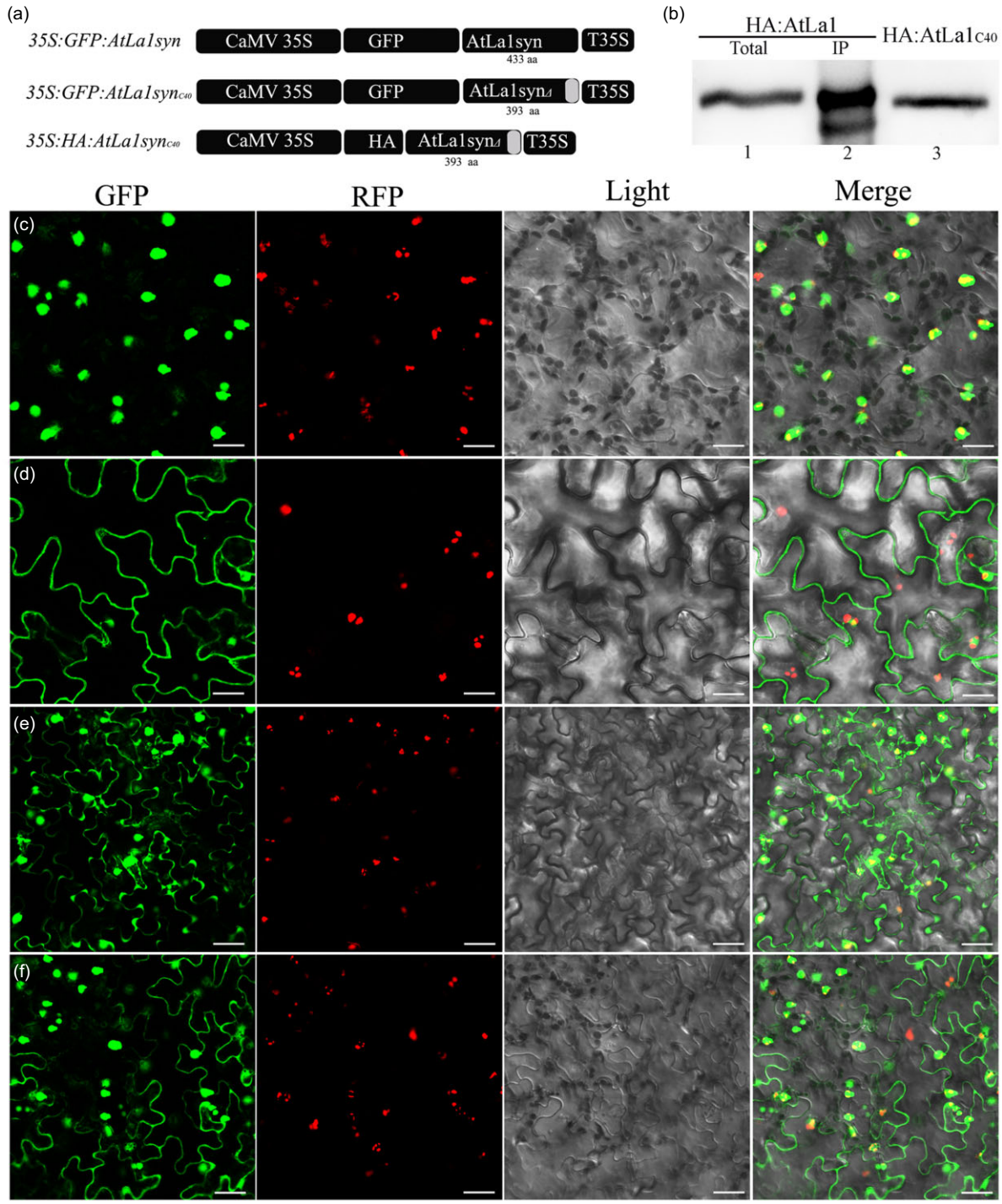

Figure 6. Environmental hazards enhance the nuclear-to-cytoplasmic translocation of the AtLa1 protein. (a) A diagram of the *35S$_{pro}$*:green fluorescent protein (*GFP*):*AtLa1$_{syn}$* construct, the *35S$_{pro}$:GFP:AtLa1$_{synC40}$* construct, and the *35S$_{pro}$:HA:AtLa1$_{synC40}$* construct with the C-terminal truncation of 40 amino acids (grey box). The intact AtLa1 protein contains 433 amino acids. (b) Cleavage of the C-terminus of the HA:AtLa1 protein in *35S$_{pro}$:HA:AtLa1$_{syn}$* plants. Lane 1: The intact HA:AtLa1 protein detected in total protein prepared from *35S$_{pro}$:HA:AtLa1$_{syn}$* plants; lane 2: the cleaved HA:AtLa1 protein (lower band) immunoprecipitated from the cytoplasmic fraction prepared from *35S$_{pro}$:HA:AtLa1$_{syn}$* plants; lane 3: the truncated HA:AtLa1$_{C40}$ protein lacking the 40 C-terminal amino acids prepared from *35S$_{pro}$:HA:AtLa1$_{synC40}$* plants. (c) The GFP:AtLa1 protein colocalized with the Collin:RFP protein in the nucleus of epidermal cells from *35S$_{pro}$:GFP:AtLa1$_{syn}$ 35S$_{pro}$:Collin:RFP* plants. (d) The GFP:AtLa1$_{C40}$ protein freely localized in the cytoplasm of epidermal cells from *35S$_{pro}$:GFP:AtLa1$_{synC40}$ 35S$_{pro}$:Collin:RFP* plants. (e, f) The GFP:AtLa1 protein can translocate from the nucleus to the cytoplasm in some epidermal cells from *35S$_{pro}$:GFP:AtLa1$_{syn}$ 35S$_{pro}$:Collin:RFP* plants subjected to ultraviolet (UV)-B irradiation (e) or 1000 mg L^{-1} zeocin treatment (f). Scale bars = 10 μm in c, d, e and f.

40 C-terminal amino acids (Fig. 6a). The GFP:AtLa1$_{C40}$ protein was randomly distributed in the cytoplasm (Fig. 6d), suggesting that the C-terminus of the AtLa1 protein contains a nuclear localization signal peptide, similar to the human La protein.

The nuclear-to-cytoplasmic translocation of the human La protein is enhanced by exposure to environmental hazards, such as UV irradiation and DNA damaging reagents (Ayukawa *et al*. 2000). We also found that the GFP:AtLa1 protein was clearly distributed in the cytoplasm of epidermal cells in *35S$_{pro}$:GFP:AtLa1syn 35S$_{pro}$:Collin:RFP* plants 24 h after mild UV-B irradiation or by the radiomimetic drug zeocin treatment (Fig. 6e & f). By contrast, the localization of the Collin:RFP protein was not affected at the same time (Fig. 6e & f). Furthermore, the frequencies of the nuclear-to-cytoplasmic translocation of GFP:AtLa1 protein in epidermal cells were significantly increased in the presence of increasing amounts of zeocin (Supporting Information Fig. S5). Taken together, these results suggest that only a small amount of AtLa1 protein can be transported to cytoplasm under optimal conditions, but the nuclear-to-cytoplasmic translocation of the AtLa1 protein is enhanced by exposure to environmental hazards.

Environmental hazards enhance *WUS* IRES-dependent translation

To examine whether the enhanced nuclear-to-cytoplasmic translocation of the AtLa1 protein caused by exposure to environmental hazards might accelerate *WUS* IRES-dependent translation, we created a transgenic plant carrying the dicistronic *35S$_{pro}$:GFP-WUS 5'UTR-RFP* construct, which expresses a red fluorescent protein (RFP) under the control of *WUS* 5'UTR (Fig. 7a). GFP but not RFP clearly accumulated in the epidermal cells of all independent lines (Fig. 7b). RFP did not clearly accumulate, possibly because only a small amount of endogenous AtLa1 protein can traffic to cytoplasm and fails to modulate the efficient translation of the RFP in the epidermal cells. As the *WUS* IRES-dependent translation of FLuc was clearly detected in epidermal cells (Fig. 5c), these results suggested that the fluorescent protein assay is not as sensitive as luciferase assay, which is consistent with an earlier report (Choy *et al*. 2003). The *35S$_{pro}$:GFP-WUS 5'UTR-RFP* plants were subjected to UV-B irradiation or zeocin treatment to enhance the nuclear-to-cytoplasmic translocation of the endogenous AtLa1 protein. RFP levels were significantly increased in the epidermal cells 24 h after UV-B irradiation or zeocin treatment (Fig. 7c & d), suggesting that the *WUS* IRES-dependent translation of RFP is enhanced by exposure to environmental hazards.

Modulation of the *WUS-CLV3* loop in the SAM by exposure to environmental hazards

The expression of *WUS* and *CLV3* was further examined in the SAM of *Arabidopsis* under environmental hazards. The GFP:GUS fusion protein clearly accumulated in the organizing centre, but not the outermost stem cell layers in the SAM of *WUS$_{pro}$:GFP:GUS* seedlings (Fig. 8a). This result suggests that the GFP:GUS fusion protein is not mobile, in contrast to the WUS:GFP fusion protein (Yadav *et al*. 2011). When the *WUS$_{pro}$:GFP:GUS* seedlings were germinated and grown on medium containing 20 mg L^{-1} zeocin for 4 d, the GFP:GUS fusion protein expanded to the outermost cell layers of the SAM (Fig. 8b). Because the GFP:GUS fusion protein was not mobile, these results suggest that the distribution of the expression of the *WUS* gene is expanded following exposure to environmental hazards. Consistent with this result, the levels of *GFP:GUS* mRNA and *WUS* mRNA were significantly increased in the *WUS$_{pro}$:GFP:GUS* seedlings subjected to zeocin treatment (Fig. 8e). Furthermore, the expression of some other stem cell-related genes was also regulated by zeocin treatment in qRT-PCR analysis (Supporting Information Fig. S6).

As in earlier reports on the *CLV3* expression pattern (Fletcher *et al*. 1999; Lenhard & Laux 2003), the GFP:GUS fusion protein in the SAM of *CLV3$_{pro}$:GFP:GUS* seedlings mainly accumulated in the outermost cell layers (Fig. 8c). When the *CLV3$_{pro}$:GFP:GUS* seedlings were germinated and grown on medium containing 20 mg L^{-1} zeocin for 4 d, the levels of *GFP:GUS* mRNA drived by *CLV3* promoter and the endogenous *CLV3* mRNA were significantly increased (Fig. 8e). The possible reason is that zeocin treatment increases the expression level of WUS, which acts as an upstream activator of *CLV3* gene (Yadav *et al*. 2011). However, the expression of the GFP:GUS fusion protein was significantly decreased in the SAM in these plants following zeocin treatment (Fig. 8d). These results indicate that the *CLV3* 5'UTR-directed translation might be 5′-terminal cap-dependent and inhibited by environmental hazards. This is consistent with the earlier reports that the cap-dependent translation of most cellular mRNAs is inhibited by environmental hazards (Rhoads & Lamphear 1995; Song *et al*. 1995; Hellen & Sarnow 2001).

The effect of zeocin treatment on the expression of endogenous WUS protein in *WUS$_{pro}$:WUS:GFP CLV3$_{pro}$:mCherry:NLS wus* plants was further explored. Consistent with the results shown earlier, zeocin treatment also increased the expression level of WUS:GFP protein and decreased the expression level of mCherry:NLS protein in the SAM of this plant (Supporting Information Fig. S7). Taken together, *WUS* expression was released from the feedback inhibition loop imposed by *CLV3* and expanded into the stem cell region following exposure to environmental hazards.

WUS protein maintains SAM development following exposure to environmental hazards

We further examined the effects of environmental hazards on the development of the SAM in *35S$_{pro}$:AtLa1 WUS$_{pro}$:GFP:GUS* seedlings, *WUS$_{pro}$:GFP:GUS* seedlings and *35S$_{pro}$:HA:AtLa1$_{syn}$ WUS$_{pro}$:GFP:GUS* seedlings that express the AtLa1 protein at different levels. The *35S$_{pro}$:AtLa1 WUS$_{pro}$:GFP:GUS* seedlings showed a transient growth cessation during the first week after germination because of the co-suppression of *AtLa1* gene and then developed true

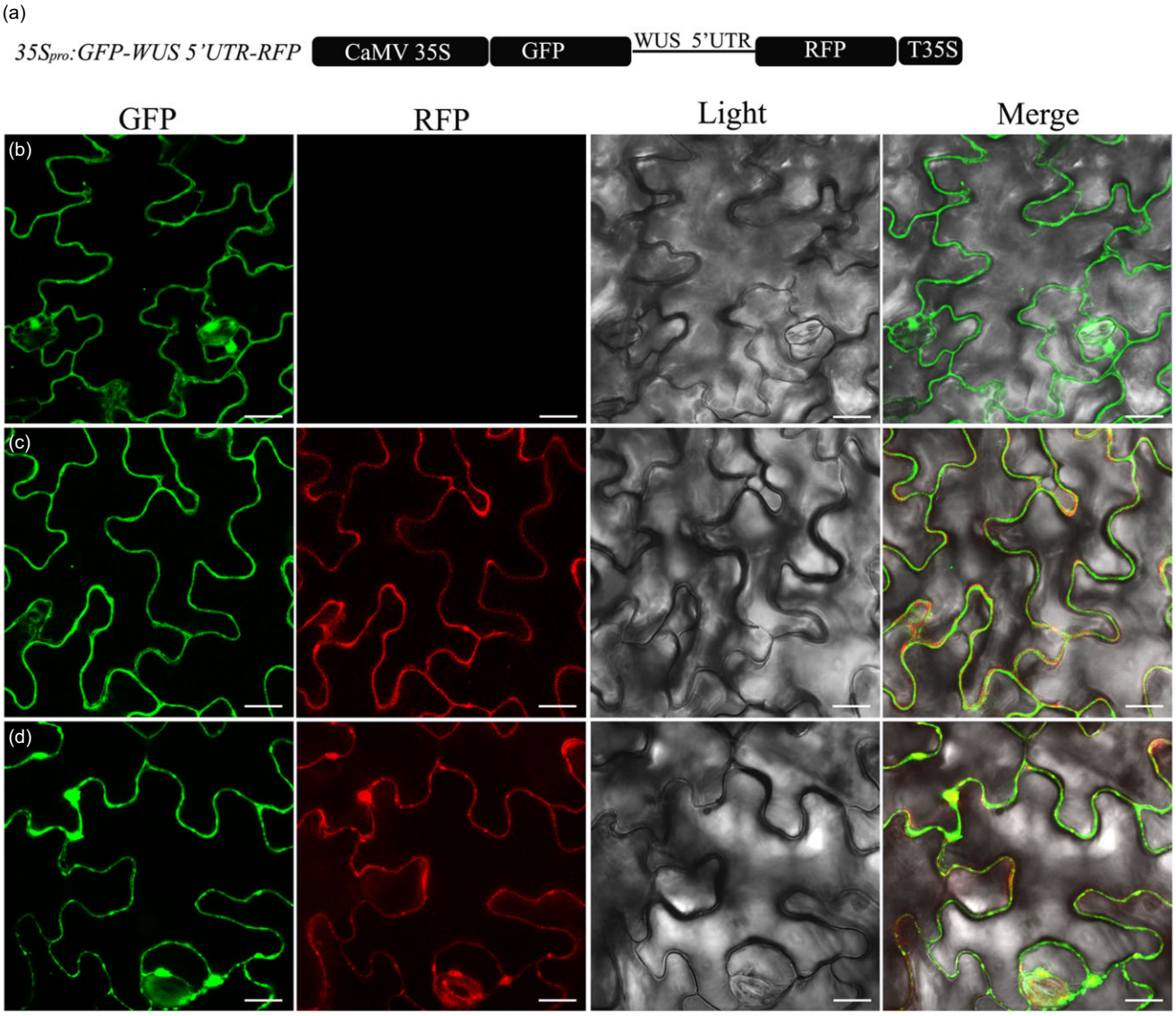

Figure 7. Environmental hazards enhance *WUS* internal ribosomal entry site (IRES)-dependent translation. (a) A diagram of the *35S$_{pro}$:*green fluorescent protein (*GFP*)-*WUS 5'UTR*-red fluorescent protein (RFP) construct. (b) GFP, but not RFP, was detected in the epidermal cells of *35S$_{pro}$:GFP-WUS 5'UTR-RFP* plants. (c,d) RFP expression was significantly increased in the epidermal cells of *35S$_{pro}$:GFP-WUS 5'UTR-RFP* plants subjected to ultraviolet (UV)-B irradiation (c) or 1000 mg L^{-1} zeocin treatment (d). Scale bars = 10 μm in b, c and d.

leaves normally. The differentiation of true leaves in *35S$_{pro}$:AtLa1 WUS$_{pro}$:GFP:GUS* seedlings was significantly repressed when grown on the medium containing 20 mg L^{-1} zeocin for 2 weeks of culture. By contrast, all of the *WUS$_{pro}$:GFP:GUS* seedlings and *35S$_{pro}$:HA:AtLa1$_{syn}$ WUS$_{pro}$:GFP:GUS* seedlings still developed true leaves on the same medium (Fig. 9a). When zeocin concentrations were increased to 40 or 60 mg L^{-1}, the percentages of the *35S$_{pro}$:HA:AtLa1$_{syn}$ WUS$_{pro}$:GFP:GUS* seedlings that produced true leaves was higher than that of the *35S$_{pro}$:AtLa1 WUS$_{pro}$:GFP:GUS* seedlings and *WUS$_{pro}$:GFP:GUS* seedlings (Fig. 9a). Consistently, the GFP:GUS fusion protein level was gradually increased in the SAM of *35S$_{pro}$:AtLa1 WUS$_{pro}$:GFP:GUS* seedlings, *WUS$_{pro}$:GFP:GUS* seedlings and *35S$_{pro}$:HA:AtLa1$_{syn}$ WUS$_{pro}$:GFP:GUS* seedlings grown on medium containing zeocin, as demonstrated by GUS staining (Fig. 9b). These results suggest that higher AtLa1 protein levels induce higher WUS expression levels, which in turn support a more sustainable development of the SAM when environmental hazards are present. Accordingly, *35S$_{pro}$:HA:WUS* seedlings exhibiting a weak phenotype and normal seed setting developed true leaves on the medium containing 60 mg L^{-1} zeocin after 3 weeks of culture, while the WT seedlings did not (Fig. 9c).

DISCUSSION

AtLa1 protein initiates translation of *WUS* mRNA

The role of the La protein in the processing and metabolism of RNAs has been extensively studied in mammalian cells

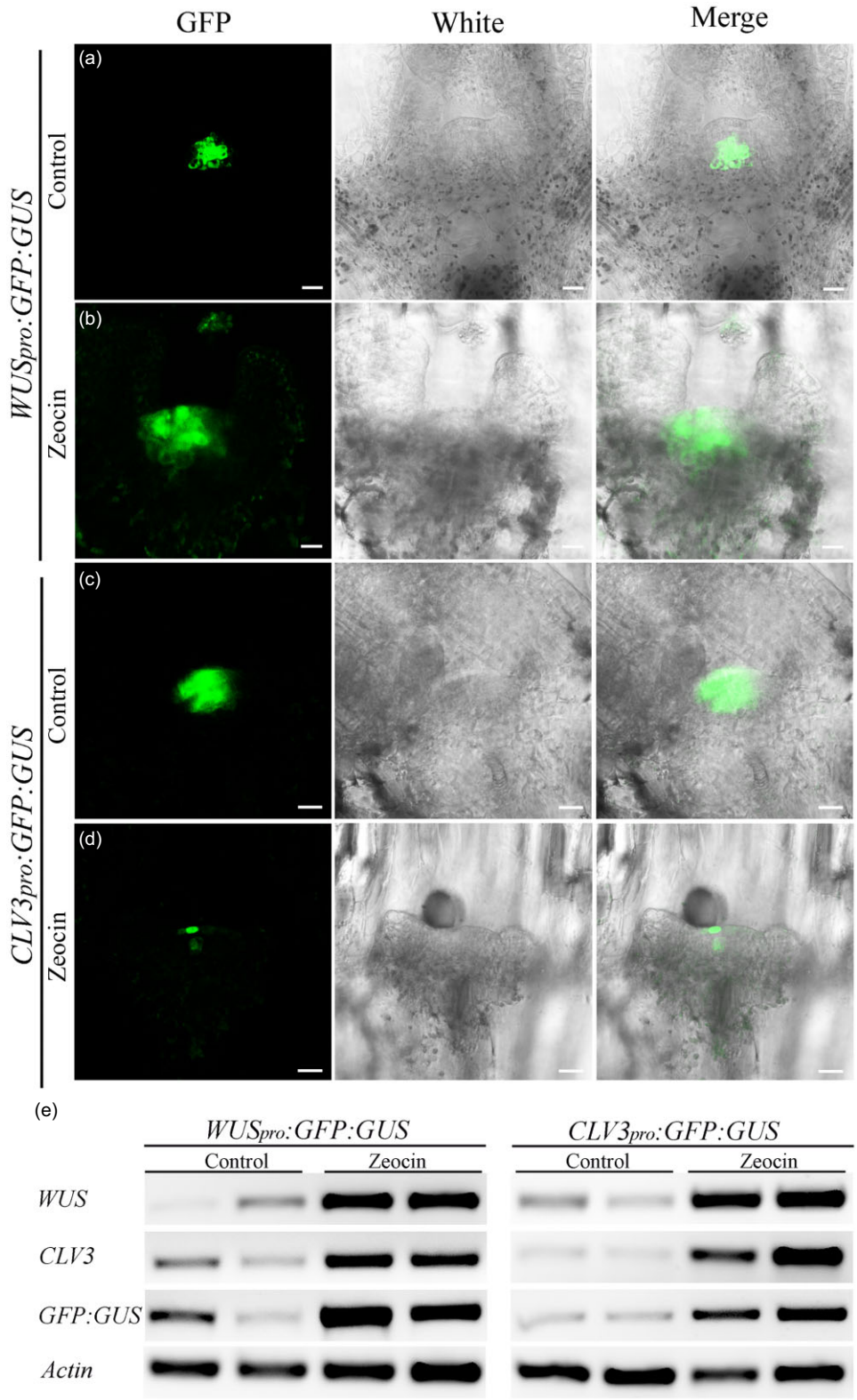

Figure 8. Zeocin treatment enhances *WUS* expression but represses *CLV3* 5′UTR-directed translation in the shoot apical meristem (SAM). (a, b) The expression of the green fluorescent protein (GFP):β-glucuronidase (GUS) fusion protein was significantly increased in the SAM of WUS_{pro}*:GFP:GUS* seedlings subjected to zeocin treatment (b) compared with control plants (a). (c, d) The expression of the GFP:GUS fusion protein was significantly decreased in the SAM of $CLV3_{pro}$*:GFP:GUS* seedlings subjected to zeocin treatment (d) compared with control plants (c). Scale bars = 20 μm in a, b, c and d. (e) Zeocin treatment increased the expression levels of *WUS* mRNA, *CLV3* mRNA, and *GFP:GUS* mRNA in WUS_{pro}*:GFP:GUS* and $CLV3_{pro}$*:GFP:GUS* plants. Two independent samples were assayed.

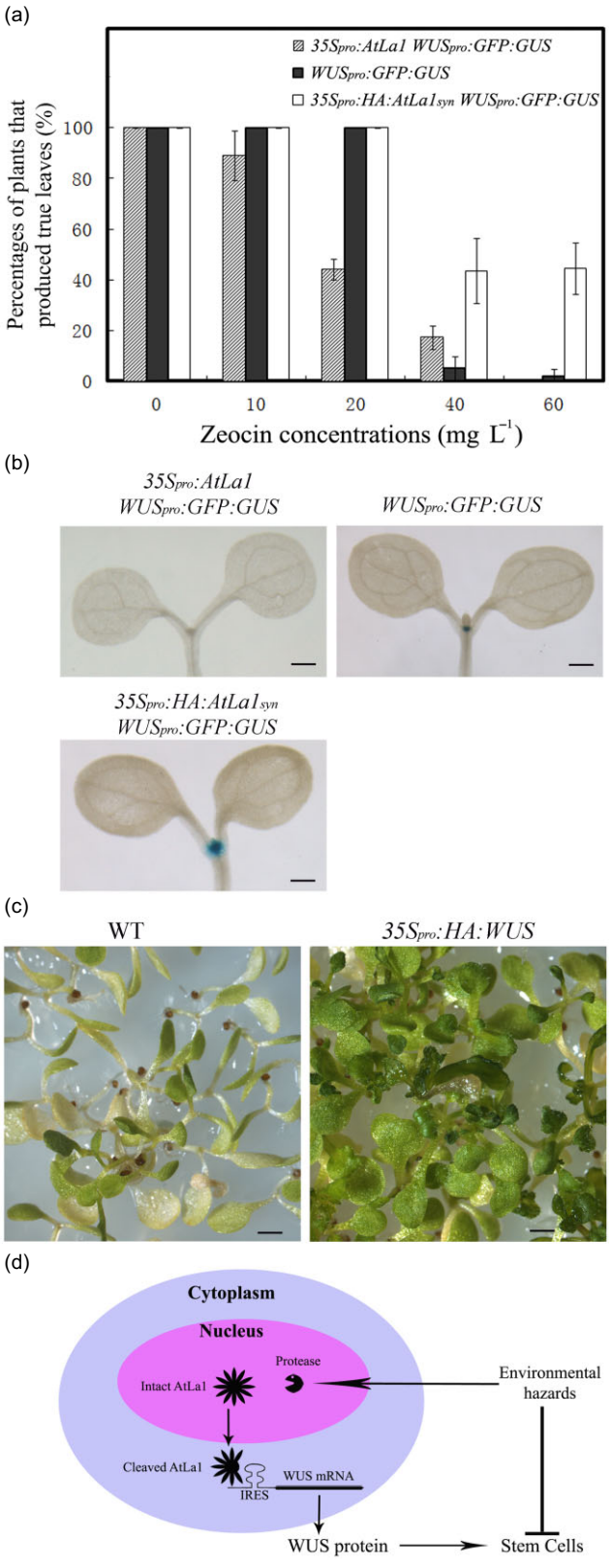

Figure 9. The WUS protein maintains shoot apical meristem (SAM) development under environmental hazards. (a) The percentages of different transgenic seedlings that produced true leaves on medium containing different concentrations of zeocin. Data presented are mean ± SE, $n = 3$. (b) The expression of the green fluorescent protein (GFP):β-glucuronidase (GUS) protein gradually increased in the SAM of $35S_{pro}$:*AtLa1* WUS_{pro}:*GFP:GUS* seedlings, WUS_{pro}:*GFP:GUS* seedlings, and $35S_{pro}$:*HA:AtLa1*$_{syn}$ WUS_{pro}:*GFP:GUS* seedlings subjected to zeocin treatment, as demonstrated by GUS staining. (c) $35S_{pro}$:*HA:WUS* seedlings, but not wild-type (WT) seedlings, produced true leaves on medium containing 60 mg L^{-1} zeocin. Scale bars = 2 mm in b, and 5 mm in c. (d) A proposed model for the modulation of stem cell homeostasis by the AtLa1 protein under conditions of environmental stress. Environmental hazards cause damage to stem cells, but also stimulate the cleavage of the AtLa1 protein by an unknown protease in the nucleus. Then, cleaved AtLa1 translocates to the cytoplasm and enhances the translation of *WUS* mRNA. The increase in WUS protein promotes the proliferation of stem cells and increases the tolerance of the SAM to environmental hazards.

(Wolin & Cedervall 2002). Fleurdépine *et al.* (2007) reported that the AtLa1 protein plays an important role in the embryogenesis of *Arabidopsis*. Consistent with this report, we determined that the AtLa1 protein is highly expressed during embryogenesis (Fig. 1). In this work, the function of the AtLa1 protein in the SAM maintenance was extensively investigated. When *AtLa1* expression was disrupted, the post-embryonic development of transgenic plants was severely repressed because the translation of *WUS* mRNA is inhibited (Figs. 2 & 3). The AtLa1 protein binds to the 5'UTR of *WUS* mRNA and regulates its translation in a dose-dependent manner, as demonstrated using both *in vivo* and *in vitro* assays (Figs. 4 & 5). Translation of *WUS* mRNA is thus strictly regulated by the amount of AtLa1 protein. The N-terminal domain of the human La protein, which consists of a La motif and an RRM1 motif, is sufficient for RNA binding (Bayfield *et al.* 2010; Naeeni *et al.* 2012). However, the truncated AtLa1 protein containing only the RRM2 domain can bind to the *WUS* 5'UTR (Fig. 4c). Therefore, the function based on the structure of the AtLa1 protein is not completely conserved in *Arabidopsis* compared with La proteins in other species. Our results also suggested that the AtLa1 protein might be cleaved at its C-terminus through a mechanism different from that observed for the human La protein (Ayukawa *et al.* 2000). Consistent with the results of an earlier report (Fleurdépine *et al.* 2007), the intact GFP:AtLa1 protein was mainly localized to the nucleus (Fig. 6c). Only a small amount of AtLa1 protein can traffic to cytoplasm after the cleavage in its C-terminus (Fig. 6b), similar to the human La protein and *Xenopus* La protein (Ayukawa *et al.* 2000; Cardinali *et al.* 2003). These results indicate that the C-terminus is involved in the nuclear and cytoplasmic activities of the AtLa1 protein. The universal expression of *AtLa1* gene in *Arabidopsis* indicates that AtLa1 protein might also regulate the translation of other mRNAs in response to environmental stresses, which remains to be investigated.

Environmental hazards enhance the IRES-dependent translation of *WUS* mRNA

Translation of most eukaryotic mRNAs involves a 5′-terminal cap-dependent mechanism termed 'ribosome scanning' (Kozak 1989). However, some mRNAs contain an IRES in the 5'UTR that can efficiently initiate cap-independent translation (Supporting Information Fig. S8), particularly under conditions of environmental stress during which the translation of most mRNAs is repressed (Hellen & Sarnow 2001). The IRES-dependent translation was usually initiated by some special cellular RNA-binding factors, such as La protein, the pyrimidine tract–binding protein (PTB), and the poly (rC) binding protein-2 (PCBP-2) (Blyn *et al*. 1996, 1997; Pestova *et al*. 1996; Kaminski & Jackson 1998; Holcik & Korneluk 2000; Kim *et al*. 2001; Costa-Mattioli *et al*. 2004). Previous studies showed that several plant viral RNAs also use IRES-dependent translation (Jaag *et al*. 2003; Dorokhov *et al*. 2006; Karetnikov & Lehto 2007). Maize *HSP101* mRNA is the only plant cellular mRNA that has been shown to utilize the IRES-dependent translation mechanism. The translation of the *HSP101* mRNA in maize is mediated by the IRES element in its 5'UTR and enhanced by heat stress (Dinkova *et al*. 2005), while cap-dependent translation of most cellular mRNAs is inhibited by heat stress (Rhoads & Lamphear 1995; Song *et al*. 1995). Our studies using dicistronic constructs demonstrated that the 5'UTR of *WUS* mRNA contains an IRES and mediates cap-independent translation under the control of AtLa1 protein (Fig. 5). Environmental hazards promoted the nuclear-to-cytoplasmic translocation of the AtLa1 protein as that of human La protein (Fig. 6), which further enhanced *WUS* IRES-dependent translation (Fig. 7). Therefore, the AtLa1 protein mediates a direct pathway by which environmental hazards modulate the translation of *WUS* mRNA.

Modulation of stem cell homeostasis in SAM following exposure to environmental hazards

Arabidopsis stem cells are hypersensitive to the DNA damage caused by UV radiation or the radiomimetic drug zeocin (Fulcher & Sablowski 2009; Furukawa *et al*. 2010). Stem cell niches must cope with environmental hazards and maintain stem cell homeostasis to ensure normal development and protect the germline. In *Arabidopsis*, the WUS protein specifies stem cell fate in the central zone of the SAM (Laux *et al*. 1996; Mayer *et al*. 1998; Schoof *et al*. 2000). Accordingly, the inducible activation of the *WUS* gene within the central zone results in proliferation of stem cells (Yadav *et al*. 2010). By contrast, the transient down-regulation of the *CLV3* gene also induces the accumulation of more stem cells in the SAM (Reddy & Meyerowitz 2005). When *Arabidopsis* seedlings were subjected to zeocin treatment, both the transcription of *WUS* mRNA and the *WUS* IRES-dependent translation were significantly enhanced (Figs. 7d, 8b & e). However, *CLV3* 5'UTR-directed translation was significantly repressed by zeocin treatment (Fig. 8d). Although *CLV3* 5'UTR-directed translation was not extensively investigated in this study, our results indicate that the translation of *CLV3* might employ the 5′-terminal cap-dependent mechanism and is inhibited under environmental hazards. Therefore, environmental hazards may disrupt the feedback loop between *WUS* and *CLV3* because *WUS* and *CLV3* mRNAs use IRES-dependent translation and cap-dependent translation, respectively. The increased levels of the WUS protein in combination with the decreased levels of the CLV3 protein should promote the proliferation of stem cells, thereby providing a basis for sustainable development following exposure to environmental hazards and the possibility of recovery from environmental hazards when the external environment becomes optimal. Based on these results, we propose a model for interpreting how the stem cell niche in *Arabidopsis* responds to environmental hazards in which the translation of *WUS* mRNA is enhanced via the AtLa1 protein (Fig. 9d). Whether the WUS protein also enhances the tolerance of stem cells to environmental hazards by regulating the repair of DNA damage and metabolic processes remains to be elucidated.

ACKNOWLEDGMENTS

We acknowledge Prof. Jan Lohmann for providing WUS_{pro}*:WUS:GFP* $CLV3_{pro}$*:mCherry:NLS wus* seeds. This work was supported by grants from the Ministry of Science and Technique of China (2013CB967302), the National Natural Science Foundation of China (30870209) and the Fundamental Research Funds for the Central Universities (2011121027). No conflict of interest was declared.

REFERENCES

Ayukawa K., Taniguchi S., Masumoto J., Hashimoto S., Sarvotham H., Hara A., . . . Sagara J. (2000) La autoantigen is cleaved in the COOH terminus and loses the nuclear localization signal during apoptosis. *The Journal of Biological Chemistry* **275,** 34465–34470.

Bayfield M.A., Yang R. & Maraia R.J. (2010) Conserved and divergent features of the structure and function of La and La-related proteins (LARPs). *Biochimica et Biophysica Acta* **1799,** 365–378.

Biedermann S. & Hellmann H. (2010) The DDB1a interacting proteins ATCSA-1 and DDB2 are critical factors for UV-B tolerance and genomic integrity in *Arabidopsis thaliana*. *The Plant Journal* **62,** 404–415.

Blyn L.B., Swiderek K.M., Richards O., Stahl D.C., Semler B.L. & Ehrenfeld E. (1996) Poly(rC) binding protein 2 binds to stem-loop IV of the poliovirus RNA 5′ noncoding region: identification by automated liquid chromatography-tandem mass spectrometry. *Proceedings of the National Academy of Sciences of the United States of America* **93,** 11115–11120.

Blyn L.B., Towner J.S., Semler B.L. & Ehrenfeld E. (1997) Requirement of poly(rC) binding protein 2 for translation of poliovirus RNA. *Journal of Virology* **71,** 6243–6246.

Brand U., Fletcher J.C., Hobe M., Meyerowitz E.M. & Simon R. (2000) Dependence of stem cell fate in *Arabidopsis* on a feedback loop regulated by CLV3 activity. *Science* **289,** 617–619.

Bray C.M. & West C.E. (2005) DNA repair mechanisms in plants: crucial sensors and effectors for the maintenance of genome integrity. *The New Phytologist* **168,** 511–528.

Broekhuis C.H., Neubauer G., van der Heijden A., Mann M., Proud C.G., van Venrooij W.J. & Pruijn G.J. (2000) Detailed analysis of the phosphorylation of the human La (SS-B) autoantigen.(De) phosphorylation does not affect its subcellular distribution. *Biochemistry* **39,** 3023–3033.

Cardinali B., Carissimi C., Gravina P. & Pierandrei-Amaldi P. (2003) La protein is associated with terminal oligopyrimidine mRNAs in actively translating polysomes. *The Journal of Biological Chemistry* **278,** 35145–35151.

Chakshusmathi G., Kim S.D., Rubinson D.A. & Wolin S.L. (2003) A La protein requirement for efficient pre-tRNA folding. *The EMBO Journal* **22,** 6562–6572.

Choy G., O'Connor S., Diehn F.E., Costouros N., Alexander H.R., Choyke P. & Libutti S.K. (2003) Comparison of noninvasive fluorescent and bioluminescent small animal optical imaging. *Biotechniques* **35,** 1022–1026, 1028–1030.

Clark S.E., Williams R.W. & Meyerowitz E.M. (1997) The *CLAVATA1* gene encodes a putative receptor kinase that controls shoot and floral meristem size in *Arabidopsis*. *Cell* **89,** 575–585.

Clough S.J. & Bent A.F. (1998) Floral dip: a simplified method for *Agrobacterium*-mediated transformation of *Arabidopsis thaliana*. *The Plant Journal* **16,** 735–743.

Collier S., Pendle A., Boudonck K., van Rij T., Dolan L. & Shaw P. (2006) A distant coilin homologue is required for the formation of cajal bodies in *Arabidopsis*. *Molecular Biology of the Cell* **17,** 2942–2951.

Copela L.A., Chakshusmathi G., Sherrer R.L. & Wolin S.L. (2006) The La protein functions redundantly with tRNA modification enzymes to ensure tRNA structural stability. *RNA (New York, N.Y.)* **12,** 644–654.

Costa-Mattioli M., Svitkin Y. & Sonenberg N. (2004) La autoantigen is necessary for optimal function of the poliovirus and hepatitis C virus internal ribosome entry site *in vivo* and *in vitro*. *Molecular and Cellular Biology* **24,** 6861–6870.

Dinkova T.D., Zepeda H., Martínez-Salas E., Martínez L.M., Nieto-Sotelo J. & Jiménez E.S. (2005) Cap-independent translation of maize Hsp101. *The Plant Journal* **41,** 722–731.

Dorokhov Y.L., Ivanov P.A., Komarova T.V., Skulachev M.V. & Atabekov J.G. (2006) An internal ribosome entry site located upstream of the crucifer-infecting tobamovirus coat protein (CP) gene can be used for CP synthesis *in vivo*. *The Journal of General Virology* **87,** 2693–2697.

Fletcher J.C., Brand U., Running M.P., Simon R. & Meyerowitz E.M. (1999) Signaling of cell fate decisions by CLAVATA3 in *Arabidopsis* shoot meristems. *Science* **283,** 1911–1914.

Fleurdépine S., Deragon J.-M., Devic M., Guilleminot J. & Bousquet-Antonelli C. (2007) A *bona fide* La protein is required for embryogenesis in *Arabidopsis thaliana*. *Nucleic Acids Research* **35,** 3306–3321.

Fok V., Friend K. & Steitz J.A. (2006) Epstein–Barr virus noncoding RNAs are confined to the nucleus, whereas their partner, the human La protein, undergoes nucleocytoplasmic shuttling. *The Journal of Cell Biology* **173,** 319–325.

Fulcher N. & Sablowski R. (2009) Hypersensitivity to DNA damage in plant stem cell niches. *Proceedings of the National Academy of Sciences of the United States of America* **106,** 20984–20988.

Furukawa T., Curtis M.J., Tominey C.M., Duong Y.H., Wilcox B.W., Aggoune D., . . . Britt A.B. (2010) A shared DNA-damage-response pathway for induction of stem-cell death by UVB and by gamma irradiation. *DNA Repair* **9,** 940–948.

Hellen C.U. & Sarnow P. (2001) Internal ribosome entry sites in eukaryotic mRNA molecules. *Genes & Development* **15,** 1593–1612.

Holcik M. & Korneluk R.G. (2000) Functional characterization of the X-linked inhibitor of apoptosis (XIAP) internal ribosome entry site element: role of La autoantigen in XIAP translation. *Molecular and Cellular Biology* **20,** 4648–4657.

Horke S., Reumann K., Schulze C., Grosse F. & Heise T. (2004a) The La motif and the RNA recognition motifs of human La autoantigen contribute individually to RNA recognition and subcellular localization. *The Journal of Biological Chemistry* **279,** 50302–50309.

Horke S., Reumann K., Schweizer M., Will H. & Heise T. (2004b) Nuclear trafficking of La protein depends on a newly identified nucleolar localization signal and the ability to bind RNA. *The Journal of Biological Chemistry* **279,** 26563–26570.

Inada M. & Guthrie C. (2004) Identification of Lhp1p-associated RNAs by microarray analysis in *Saccharomyces cerevisiae* reveals association with coding and noncoding RNAs. *Proceedings of the National Academy of Sciences of the United States of America* **101,** 434–439.

Jaag H.M., Kawchuk L., Rohde W., Fischer R., Emans N. & Prüfer D. (2003) An unusual internal ribosomal entry site of inverted symmetry directs expression of a potato leafroll polerovirus replication-associated protein. *Proceedings of the National Academy of Sciences of the United States of America* **100,** 8939–8944.

Jefferson R.A., Kavanagh T.A. & Bevan M.W. (1987) GUS fusions: beta-glucuronidase as a sensitive and versatile gene fusion marker in higher plants. *The EMBO Journal* **6,** 3901–3907.

Jeong S., Trotochaud A.E. & Clark S.E. (1999) The *Arabidopsis CLAVATA2* gene encodes a receptor-like protein required for the stability of the CLAVATA1 receptor-like kinase. *The Plant Cell* **11,** 1925–1934.

Kadaba S., Wang X. & Anderson J.T. (2006) Nuclear RNA surveillance in *Saccharomyces cerevisiae*: Trf4p-dependent polyadenylation of nascent hypomethylated tRNA and an aberrant form of 5S rRNA. *RNA (New York, N.Y.)* **12,** 508–521.

Kaminski A. & Jackson R.J. (1998) The polypyrimidine tract binding protein (PTB) requirement for internal initiation of translation of cardiovirus RNAs is conditional rather than absolute. *RNA (New York, N.Y.)* **4,** 626–638.

Karetnikov A. & Lehto K. (2007) The RNA2 5'leader of Blackcurrant reversion virus mediates efficient *in vivo* translation through an internal ribosomal entry site mechanism. *The Journal of General Virology* **88,** 286–297.

Kayes J.M. & Clark S.E. (1998) CLAVATA2, a regulator of meristem and organ development in *Arabidopsis*. *Development (Cambridge, England)* **125,** 3843–3851.

Kim Y.K., Back S.H., Rho J., Lee S.H. & Jang S.K. (2001) La autoantigen enhances translation of *BiP* mRNA. *Nucleic Acids Research* **29,** 5009–5016.

Kozak M. (1989) The scanning model for translation: an update. *The Journal of Cell Biology* **108,** 229–241.

Kufel J., Allmang C., Chanfreau G., Petfalski E., Lafontaine D.L. & Tollervey D. (2000) Precursors to the U3 small nucleolar RNA lack small nucleolar RNP proteins but are stabilized by La binding. *Molecular and Cellular Biology* **20,** 5415–5424.

Laux T., Mayer K., Berger J. & Jürgens G. (1996) The *WUSCHEL* gene is required for shoot and floral meristem integrity in *Arabidopsis*. *Development (Cambridge, England)* **122,** 87–96.

Lenhard M. & Laux T. (2003) Stem cell homeostasis in the *Arabidopsis* shoot meristem is regulated by intercellular movement of CLAVATA3 and its sequestration by CLAVATA1. *Development (Cambridge, England)* **130,** 3163–3173.

Maraia R.J. (2001) La protein and the trafficking of nascent RNA polymerase III transcripts. *The Journal of Cell Biology* **153,** F13–F18.

Maraia R.J. & Intine R.V. (2001) Recognition of nascent RNA by the human La antigen: conserved and divergent features of structure and function. *Molecular and Cellular Biology* **21,** 367–379.

Mayer K.F., Schoof H., Haecker A., Lenhard M., Jürgens G. & Laux T. (1998) Role of WUSCHEL in regulating stem cell fate in the *Arabidopsis* shoot meristem. *Cell* **95,** 805–815.

Müller R., Bleckmann A. & Simon R. (2008) The receptor kinase CORYNE of *Arabidopsis* transmits the stem cell-limiting signal CLAVATA3 independently of CLAVATA1. *The Plant Cell* **20,** 934–946.

Naeeni A.R., Conte M.R. & Bayfield M.A. (2012) RNA chaperone activity of human la protein is mediated by variant RNA recognition motif. *The Journal of Biological Chemistry* **287,** 5472–5482.

Pannone B.K., Xue D. & Wolin S.L. (1998) A role for the yeast La protein in U6 snRNP assembly: evidence that the La protein is a molecular chaperone for RNA polymerase III transcripts. *The EMBO Journal* **17,** 7442–7453.

Pestova T.V., Hellen C.U. & Shatsky I.N. (1996) Canonical eukaryotic initiation factors determine initiation of translation by internal ribosomal entry. *Molecular and Cellular Biology* **16,** 6859–6869.

Reddy G.V. & Meyerowitz E.M. (2005) Stem-cell homeostasis and growth dynamics can be uncoupled in the *Arabidopsis* shoot apex. *Science* **310,** 663–667.

Rhoads R.E. & Lamphear B.J. (1995) Cap-independent translation of heat shock messenger RNAs. *Current Topics in Microbiology and Immunology* **203,** 131–153.

Schoof H., Lenhard M., Haecker A., Mayer K.F., Jürgens G. & Laux T. (2000) The stem cell population of *Arabidopsis* shoot meristems is maintained by a regulatory loop between the *CLAVATA* and *WUSCHEL* genes. *Cell* **100,** 635–644.

Simons F.H., Broers F.J., Van Venrooij W.J. & Pruijn G.J. (1996) Characterization of cis-acting signals for nuclear import and retention of the La (SS-B) autoantigen. *Experimental Cell Research* **224,** 224–236.

Song H.J., Gallie D.R. & Duncan R.F. (1995) m7GpppG cap dependence for efficient translation of Drosophila 70-kDa heat-shock-protein (Hsp70) mRNA. *European Journal of Biochemistry/FEBS* **232,** 778–788.

Stefano J.E. (1984) Purified lupus antigen La recognizes an oligouridylate stretch common to the 3′ termini of RNA polymerase III transcripts. *Cell* **36,** 145–154.

Terzi L.C. & Simpson G.G. (2009) *Arabidopsis* RNA immunoprecipitation. *The Plant Journal* **59,** 163–168.

Wolin S.L. & Cedervall T. (2002) The LA protein. *Annual Review of Biochemistry* **71,** 375–403.
Yadav R.K., Tavakkoli M. & Reddy G.V. (2010) WUSCHEL mediates stem cell homeostasis by regulating stem cell number and patterns of cell division and differentiation of stem cell progenitors. *Development (Cambridge, England)* **137,** 3581–3589.
Yadav R.K., Perales M., Gruel J., Girke T., Jönsson H. & Reddy G.V. (2011) WUSCHEL protein movement mediates stem cell homeostasis in the *Arabidopsis* shoot apex. *Genes & Development* **25,** 2025–2030.
Yocupicio-Monroy M., Padmanabhan R., Medina F. & del Angel R.M. (2007) Mosquito La protein binds to the 3′ untranslated region of the positive and negative polarity dengue virus RNAs and relocates to the cytoplasm of infected cells. *Virology* **357,** 29–40.
Zhao Z., Andersen S.U., Ljung K., Dolezal K., Miotk A., Schultheiss S.J. & Lohmann J.U. (2010) Hormonal control of the shoot stem-cell niche. *Nature* **465,** 1089–1092.

Received 7 December 2014; received in revised form 1 March 2015; accepted for publication 2 March 2015

SUPPORTING INFORMATION

Additional Supporting Information may be found in the online version of this paper at the publisher's web-site:

Figure S1. The *AtLa1* gene regulates the expression levels of *WUS* mRNA and *CLV3* mRNA in the SAM. The expression levels of endogenous *WUS* mRNA (a–c) and *CLV3* mRNA (d–f) in the inflorescence meristem of control WUS_{pro}*:GFP:GUS* plants (a,d), one moderate line of $35S_{pro}$*:AtLa1* WUS_{pro}*:GFP:GUS* plants (b,e) and $35S_{pro}$*:anti-AtLa1* WUS_{pro}*:GFP:GUS* plants (c,f) by RNA *in situ* hybridizytion. Scale bars = 20 μm.

Figure S2. The expression of *STM* gene is not dependent on the *AtLa1* gene. The expression of the GFP:GUS protein in $35S_{pro}$*:AtLa1* STM_{pro}*:GFP:GUS* plants exhibiting growth cessation was comparable with that of the control STM_{pro}*:GFP:GUS* plants, as demonstrated by GUS staining. Scale bar = 0.7 cm.

Figure S3. An alignment between the synonymously substituted sequence of the $AtLa1_{syn}$ gene and the sequence of the *AtLa1* gene.

Figure S4. The subcellular localization of the AtLa1:GFP:GUS protein. The AtLa1:GFP:GUS protein is mainly localized to the nucleoplasm (the green ring), as well as the nuclear cavity (the green spot inside the green ring) in some root cells of $AtLa1_{pro}$*:gAtLa1:GFP:GUS* plants. Scale bars = 20 μm.

Figure S5. Zeocin treatment induced the nuclear-to-cytoplasmic translocation of GFP:AtLa1 protein in epidermal cells of $35S_{pro}$*:GFP:*$AtLa1_{syn}$ $35S_{pro}$*:Collin:RFP* plants in a dose-dependent manner. (a) The GFP:AtLa1 protein was exclusively localized to the nucleus and colocalized with the Collin:RFP protein. (b–d) The nuclear-to-cytoplasmic translocation of GFP:AtLa1 protein in epidermal cells was significantly enhanced by the treatments of zeocin at increasing concentrations. Scale bars = 40 μm in a, b, c, and d. (e) The percentages of epidermal cells with the nuclear-to-cytoplasmic translocation of GFP:AtLa1 protein was increased in the presence of zeocin at increasing concentrations.

Figure S6. Zeocin treatment regulates the expression of some stem cell-related genes in the SAM by qRT-PCR analysis. The WUS_{pro}*:GFP:GUS* plants were geminated and grown on medium containing zeocin at increasing concentrations. The expression levels of different genes after zeocin treatment were normalized to the relative gene expression level of the control WUS_{pro}*:GFP:GUS* plants in which the gene expression level was set as an arbitrary value of 1. Data presented are mean ± SE, $n = 6$.

Figure S7. Zeocin treatment increased the expression level of WUS:GFP protein and decreased the expression level of mCherry:NLS protein in the SAM of WUS_{pro}*:WUS:GFP* $CLV3_{pro}$*:mCherry:NLS wus* plants. (a) The control plants; (b) The plants germinated and grown on medium containing 10 mg L^{-1} zeocin for 7 d. Scale bars = 20 μm in a and b.

Figure S8. The diagram of 5′-terminal cap dependent translation and IRES-dependent translation. The cap-dependent translation is mediated by interaction of the m7G-cap with eIF4E. In the IRES-dependent translation, IRES forces a ribosome to directly enter the internal positions in 5'UTR, which is usually mediated by special RNA-binding proteins, such as La protein, the pyrimidine tract-binding (PTB) protein, etc.

Table S1. The primers used for semi-quantitative RT-PCR and quantitative RT-PCR.